NASA CR-72178

SEMIANNUAL REPORT

DEVELOPMENT OF FUEL CELL ELECTRODES

by

M. B. Clark and G. E. Evans

prepared for

NATIONAL AERONAUTICS AND SPACE ADMINISTRATION

December 31, 1966

CONTRACT NAS 3-9430

Technical Management
NASA Lewis Research Center
Cleveland, Ohio

Space Power Systems Division
W. A. Robertson

UNION CARBIDE CORPORATION
ELECTRONICS DIVISION
Fuel Cell Department
P. O. Box 6116
Cleveland, Ohio 44101

TABLE OF CONTENTS

LIST OF FIGURES

LIST OF TABLES

DEVELOPMENT OF FUEL CELL ELECTRODES

by M. B. Clark and G. E. Evans

Union Carbide Corporation

ABSTRACT

The applicability to aerospace requirements of a fuel cell system employing circulating liquid electrolyte and water removal via transpiration through porous electrodes is being investigated. Most of the effort covered in the present report concerns upgrading of electrode and cell performance. The best (4" x 5") cell constructed to date has operated at 200 ASF continuously for 800 hours at atmospheric pressure with a constant terminal voltage of 885 ±5 mv, with the test still in progress.

SUMMARY

Work under the present program is divided in two areas. The first area of work is the performance improvement of Union Carbide Corporation fuel cell electrodes. The effect of increased catalyst loading and improved current collection will be assessed. The goal of this effort is the development of electrodes capable of operating at 200 amperes per square foot at an initial terminal voltage of at least 0. 900 volt, and having a terminal voltage decline of not more than 0. 020 volt after 500 hours of continuous operation at 200 amperes/sq. ft. The second area of work has as its objective the evaluation of the Union Carbide system concept. The reference system shall be a nominal 5-kilowatt system operating at 29 ±2 volts with a design life of 3000 hours.

Two technical approaches are being followed in the Task 1 - Electrode Improvement phase of the program. One approach is to upgrade performance of the Union Carbide Type T-2 electrode (catalyzed carbon on porous nickel) through the use of more effective, higher catalyst loading and higher conductivity substrates to reduce cell internal resistance. A second approach is to employ highly catalyzed electrodes of the types already qualified for use in matrix-type aerospace systems, with modifications in structure to permit use in a circulating electrolyte system. Both approaches have led to useful electrodes, falling within the performance requirements established for the electrode improvement program. The best (4" x 5") cell constructed to date has operated at 200 ASF continuously for 800 hours at a constant terminal voltage of 885 ±5 mv at atmospheric pressure, with the test still in progress. This cell employs LAB-40 electrodes obtained from American Cyanamid Company.

These electrodes show excellent voltage characteristics but have occasionally failed during shutdown and restart of a test. The failure mode appears to be delamination of the Teflon facing from the active electrode as a result of thermal stress. These electrodes also show a tendency to "weepage" (formation of liquid droplets on the gas face of the electrode) which appears to be related to nonuniformity in the pore structure of the Teflon. The vendor is modifying his electrode fabrication techniques to obtain better bonding and structural uniformity in the Teflon facing, and will supply improved electrodes for testing.

Union Carbide Type T-2 electrodes (carbon on thin porous nickel) show excessive voltage degradation when used as a cell cathode at 100°C and 200 ASF. These Type T-2 electrodes, however, show excellent voltage stability when used as anodes, at potentials comparable to the LAB-40 anodes. Since the T-2 anodes remain dry on the gas face at 200 ASF (no "weepage") and are not damaged by sudden cell shutdowns, they are the preferred anode at the present time.

Experiments with pressurized cells have shown that operation at 30 psia (15 psig) adds about 30 mv to the terminal voltage at 200 ASF, giving initial terminal voltages above 0. 92 volt. Further increases in pressure to 45 and 60 psia produce relatively slight additional voltage gains. Considering problems introduced by higher pressures in the design of water removal equipment, a 30 psia design point appears to be close to optimum.

Experimental study of the effects of temperature (up to 130°C) on cell performance have shown, as expected, that higher terminal voltages can be achieved at higher temperatures. Unfortunately, at temperatures above about 100°C the electrolyte concentration must be increased to the 13 - 15 M range to maintain an acceptable vapor pressure. Operation with such concentrated electrolyte introduces major problems in the design and operation of a practical system, due to the danger of electrolyte freeze-up on cooling to ambient temperature during intermittent operation. Since high temperature operation also magnifies problems of corrosion and materials' stability, and since acceptable voltage levels can be achieved in the 90 - 100°C range, this lower temperature range has been chosen for the design study.

The materials' testing program has identified a list of materials acceptable for use in KOH electrolyte at 100°C under oxidizing conditions. It has been found that generic names for plastic materials, such as "polypropylene," "neoprene", or "Nylon" are completely inadequate designations in selecting fuel cell structural materials. For example, one grade of polypropylene disintegrates within a week

upon testing in KOH electrolyte at 100°C, while another shows no significant effects. At lease one "acceptable" material is available for fulfilling each of the functional requirements of the fuel cell structural design (e.g., framing materials, encapsulants, adhesives, gaskets, separators, sealants, etc.), but in some instances not in the desired physical form. Establishment of a list of qualified cell materials, defined with respect both to physical structure and chemical identity, is scheduled for completion within the present contract period.

Work under the Task 2 - Preliminary System Design study has just been initiated. The major effort under this Task will be the redesign in concept of certain of the components of the Union Carbide Fuel Cell system to assure compatibility with aerospace environmental requirements, in particular zero-gravity operation.

Components which require modification from previous terrestrial designs include a partitioned electrolyte-expansion tank to prevent an unstable liquid-gas interface; a liquid-gas separator to remove fortuitous gas bubbles in the electrolyte arising from dissolved reactants or peroxide decomposition; and a "wicking" type condenser to remove water from the circulating gas streams.

Several of these design problems are similar to problems previously faced and solved in the design of previous aerospace fuel cells or life-support systems. On the basis of prior experience in this field, a Subcontract is being negotiated with Garrett Corporation for design of the Thermal Control Subsystem of the proposed fuel cell system.

INTRODUCTION

Over a period of about 15 years, Union Carbide has developed a unique type of fuel cell system. While details of electrode fabrication and system component design have been modified over the years, certain central design concepts have remained constant and can be considered as defining the "Union Carbide system" design. These features include:

a) Use of a circulating aqueous KOH electrolyte as the primary means of heat removal;

b) Recirculation of one or both of the reactant gases as a means of water removal via transpiration through the porous electrodes;

c) Operation under conditions of temperature, pressure, fluid flow rates, electrolyte concentration, etc., which provide self-regulating control of the water balance;

d) Stabilization of the three-phase electrochemically active zone through control of pore geometry and wetting angle in semihydrophobic electrodes, as a means of broadening the range of gas-electrolyte differential pressures within which stable operation can be achieved;

e) Use of carbon as the principal active ingredient of the electrodes, with minimal amounts of additional catalysts, as a means of reducing cost.

For brevity in the following discussion, the design features described in a) through e) above will be referred to as the "Union Carbide system concept". The guiding philosophy in developing this system concept has been to minimize the system cost per kilowatt at a commercially useful level of power density, and to reduce the system complexity to a minimum number of (preferably static) components. Optimization with primary emphasis on cost per kilowatt, however, leads to a system of limited utility in anticipated aerospace missions, where minimum system weight becomes of critical importance. The original motivation leading to the present program was to demonstrate the applicability of the Union Carbide system concepts to aerospace mission requirements, on the basis of new trade-off criteria between system cost, performance and reliability. The major problem, in broad terms, was to develop and demonstrate a major improvement in performance (as measured by power density and energy density) without loss in reliability or life.

It was immediately apparent that it would be necessary to improve the electrode performance to permit operation at higher voltage and higher current density. A goal of 0. 900 volt terminal at 200 ASF with less than 20 mv degradation over 500 hours was selected to guide this phase of the effort. Two approaches were selected, to be followed in parallel. One approach was to start from the available Union Carbide Type-2 electrode (thin porous carbon supported on porous nickel), and to upgrade the performance by increasing the catalyst level and increasing the conductivity of the electrode. A second approach was to start with heavily catalyzed (platinum) electrodes of the types already qualified for high performance matrix cells and modify the structure so as to permit operation in circulating electrolyte cells.

It rapidly became apparent that in order to reach the electrode performance goal it would be necessary to increase the operating temperature from the 60-80°C range to the 80-100°C range. This increase in temperature improves polarization and reduces cell internal resistance, and equally important, reduces the weight of the space radiators required for heat rejection. As a consequence of this increase in temperature, however, some of the commonly employed materials of construction become marginal in stability in contact with hot KOH.

To ensure stability of materials of cell construction within the new operating conditions, a materials compatability testing study has been incorporated in the Phase 1 program. The "first screen" consists of exposure of the sample to 14 N KOH under oxidizing (atmospheric air environment) conditions at 100°C for one week. Samples are checked for dimensional or weight changes, appearance changes, loss of physical properties (embrittlement, softening, erosion, etc.). The electrolyte is also examined for evidence of chemical contamination, change in surface tension, etc.

The second phase of the present program is a preliminary design study. This re-examination of the design concepts has two aims: first, to account properly for the unique environmental conditions of aerospace missions; and second, to redesign to new internal operating conditions of temperature, pressure, and electrode polarization.

Environmental conditions of primary significance include zero-g operation, space vacuum, and launch shock, vibration, and acoustic noise specifications. Zero-gravity operation influences the design of a number of components. The normal method employed for water removal is condensation from a circulating gas stream; in the absence of gravity this requires some form of "wicking condenser"

to collect and transport liquid water in a capillary wick. Since such devices have been built and successfully tested, no major problems are anticipated beyond sizing components to match the load profile. Operation of a liquid electrolyte circulation loop under zero gravity conditions will also require some sort of device for isolation and rejection of gas bubbles in the electrolyte. Such gas bubbles can originate from differences in solubility of reactant gases in the electrolyte under thermal cycling or from decomposition of peroxides which escape the normal catalytic reaction at the electrode surface. Two approaches are being considered; in one, a highly hydrophobic porous membrane permits gas penetration while blocking liquid flow; in a second approach, a mechanical centrifuge separates gas and liquid phases. Engineering study will be required to determine which approach offers the highest reliability and lightest weight after feasibility has been established.

A third component which is significantly influenced by zero-gravity operation is the electrolyte reservoir-expansion chamber. This unit is needed to store the entire electrolyte inventory during periods of high acceleration and to accommodate electrolyte volume changes caused by thermal expansion and normal electrolyte concentration variations. Under terrestrial operating conditions the expansion tolerance is accommodated in a simple expansion tank; under zero-gravity operation a bellows or flexible bladder is required to prevent an unstable gas-liquid interface and to allow gaging of the electrolyte volume.

Operation in space vacuum introduces the requirement of establishing an absolute pressure reference rather than simply balancing pressures against an atmospheric ambient pressure. This problem has been successfully solved for several existing aerospace fuel cell types, and no difficulty is anticipated in adapting existing techniques to the present system.

FACTUAL DATA

Task 1 - Electrode Improvement.

A. Electrode Types.

Most of the test program has been centered on three general types of Union Carbide fuel cell electrodes, plus one type obtained from American Cyanamid, as described below:

1. Type-2 Electrodes: Active carbon on porous metal (a) catalyzed after fabrication, (b) carbon precatalyzed before fabrication.
2. Type-5 Electrodes: Active carbon on metal screen; Teflon-backed; carbon usually precatalyzed before fabrication.

3. American Cyanamid, LAB-40 electrodes, 40 mg Pt/cm^2 on nickel screen with Teflon backing.

4. A limited number of tests have been conducted on other experimental electrode types, including electrodes supplied by ChemCell.

Electrode improvement has consisted largely of tests directed toward:

1. Increasing the catalyst concentration, either by post-catalysis or precatalysis of the active carbon;

2. Improving the electrical conductivity by substitution of silver for nickel, and by improving the bonding of the active electrode material to the metal substrate, and

3. Reducing the electrolyte "weeping" problem (i. e. , the formation of beads of moisture on the gas side of the electrode).

B. Cell Design.

Some of our preliminary screening tests have been run in small (2. 0 cm^2) active area) cells. These are very easily assembled, consisting of electrodes mounted in injection-molded polyethylene frames which, together with other required cell components (electrolyte compartment and gas chambers), are simply clamped together and mounted on a test rack provided with means for circulating heated electrolyte. Figure 1 shows a cell of this type.

In this figure the cell is designated by the letter "B". Electrolyte is circulated through the cell by means of a "bubble-pump" using nitrogen as propellent. The bulk of the electrolyte is contained in a reservoir "G" containing a cartridge heater "H". Electrolyte is gravity fed to the cell through tube "C" and overflows from the top of the cell through tube "E, " where it flows into a tee. A constant flow of nitrogen into one side arm of the tee lifts the electrolyte back up to the reservoir.

Most of the testing has been done with larger cells with an active electrode area of 0. 125 ft^2 (4" x 4-1/2"). After some preliminary work a fairly standarized construction has been evolved. The necessity for operation temperatures to 100°C required some modifications of the usual cell type. Figure 2a shows a finished cell of the type being used at present. Figure 2b is a cell similar in all internal details, but encased in a rigid Panelite body to make it suitable for pressure testing.

In most cells the electrodes have been framed with strips of silver held in place with conductive silver-epoxy resin (Fig. 3a). This is particularly important when porous nickel is used as a backing material (Type-2 electrodes), as well as

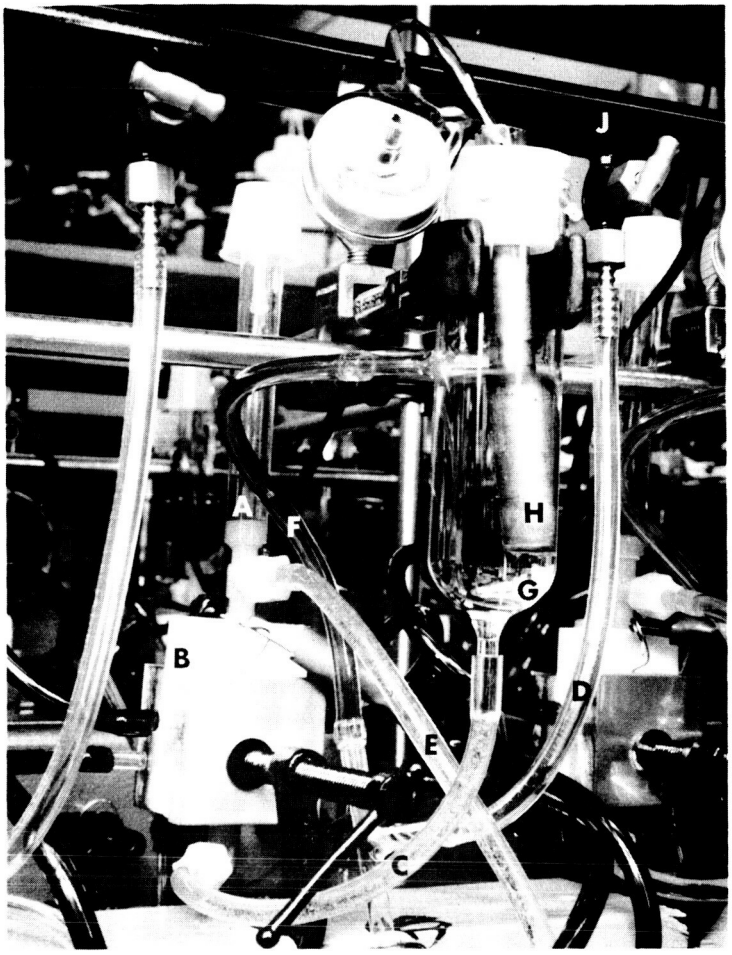

D-736

Fig. 1 - Close-up of Single Cell

A	KOH Head Tube
B	Cell
C	KOH Inlet Tube to Cell
D	Nitrogen
E	Cell Overflow
F	From Overflow to Reservoir
G	KOH Reservoir
H	Heater Sheath
J	Nitrogen Manifold

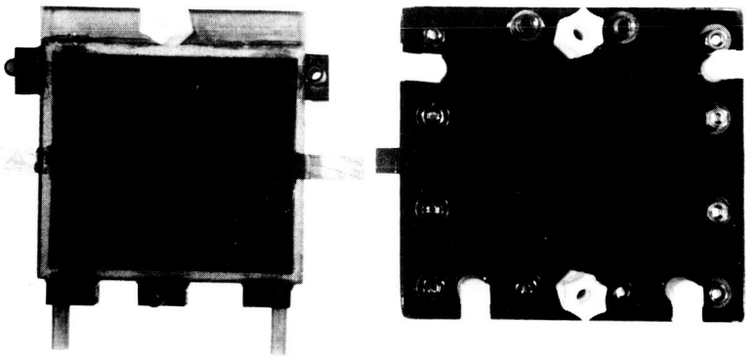

D-3144

Fig. 2a - 4" x 4-1/2" Test Cell.

Fig. 2b - 4" x 4-1/2" Pressure Cell.

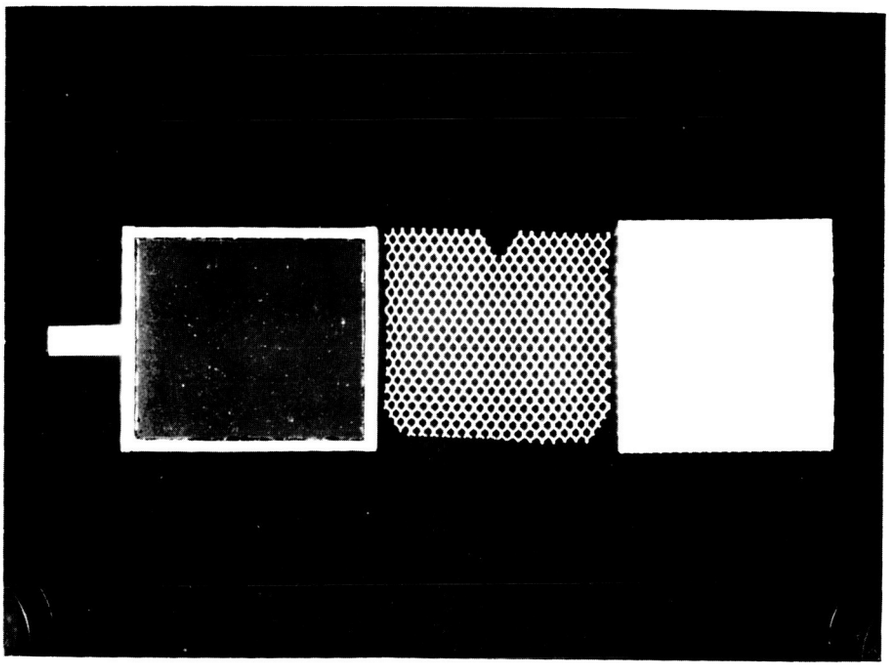

(a) (b) (c) D-3146

Fig. 3 - Test Cell Components: (a) Electrode; (b) Electrolyte Separator; (c) Gas Spacer.

with the Type-5, and the LAB-40 electrodes. A current tab in the form of a T-bar of heavy (26-mil) silver is cemented to one edge.

The best separator material found so far has been expanded Nylon (Exmet Code 10, 25-1, stabilized); see Fig. 3b. Because it has a "memory," and will contract at the higher cell temperatures used in this program, it has been necessary to anchor it at the edges with epoxy. This separator is sandwiched between the two electrodes, and the electrolyte gap of approximately 50 mils is defined by means of narrow neoprene strips cemented along the electrode edges which serve as a gasket.

The gas space behind each electrode is defined in a similar manner, but the spacer material (used to hold the electrodes firmly against the electrolyte separator) has usually been Lamport Style No. 7700 polypropylene mesh approximately 90 mils thick (Fig. 3c).

Polysulfone sheet was chosen as the outside cell casing material for most of the cells, replacing the Lucite customarily used because of the higher operating temperatures. All components are cemented together with epoxy resin, and the final cell edges "potted" with this material. Electrolyte and gas inlet and outlet ports are machined from polysulfone and cemented in place as a final step.

C. Test Facilities.

Since temperatures in the vicinity of 100°C were to be employed, modification in our usual test facilities was necessary. A simple test stand of the type used for much of this preliminary work is shown schematically in Fig. 4, and a photograph is shown in Fig. 5.

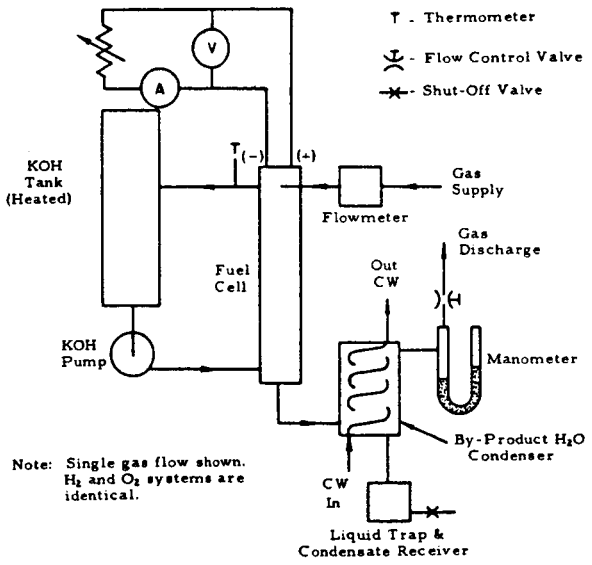

D-3122

Fig. 4 - NASA Single Cell Test, Scheme A.

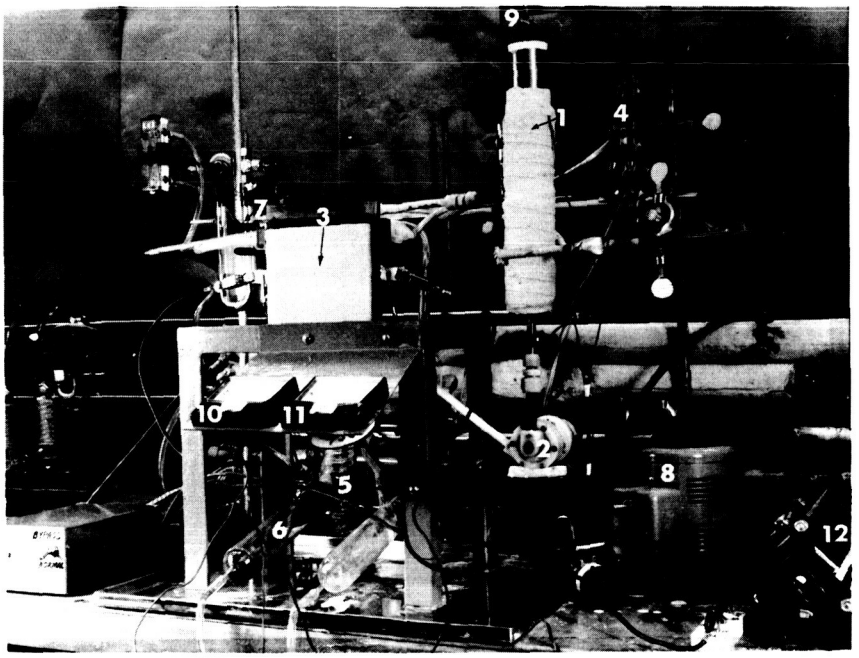

D-3119

Fig. 5 - NASA Single Cell Test, Scheme A.

In this arrangement the KOH reservoir (1) is constructed of nickel, and heated by means of heating tape. The electrolyte is circulated by means of a centrifugal pump (2), entering the bottom of the cell (3), and exiting at the top from where it returns to the reservoir. Since both gas circulating systems are identical, only one is shown in the schematic, and only the oxygen loop is identified in the photograph. Each gas first enters a flowmeter (4), then enters the cell at the top. All excess gas is purged from the system (i. e., no recirculation is provided), and leaves the cell from the bottom, the exit port being positioned diagonally across from the inlet port. The exit gas passes through a water-cooled condenser (5) which serves to remove a major portion of the water, which then collects in the condensate receiver (6). The latter also acts as a trap to detect the presence of electrolyte leakage should it occur. The exit gas finally passes through a control valve positioned on one leg of a U-tube containing mercury (7). This permits control of the gas pressure in the cell.

Also shown in the photograph is the Variac (8) used for adjusting electrolyte temperature, an electrolyte level probe (9) which automatically shuts off the hydrogen supply and puts the cell on open circuit in the event that the electrolyte level were to become dangerously low, and the components of the load circuit: voltmeter (10), ammeter (11), and rheostat (12).

In addition to five test positions of the foregoing type, one position suitable for operating at pressures up to 45 psig has been built. The schematic and photograph of this system are shown in Figs. 6 and 7. Pressure balance is achieved by simultaneous pressurization of the electrolyte with nitrogen as the hydrogen and oxygen pressures are increased. This is easily accomplished by feeding the nitrogen to one side of the diaphragm of both the hydrogen and oxygen regulators (1), Fig. 7; only one gas system is indicated in the figures. This forces the pressure of these gases to "follow" the nitrogen pressure. The hydrogen and oxygen pressures are maintained at a value slightly above that of the nitrogen by means of springs in the regulators. The electrolyte reservoir (2) and pump (3) arrangement is similar to that described for the previous system.

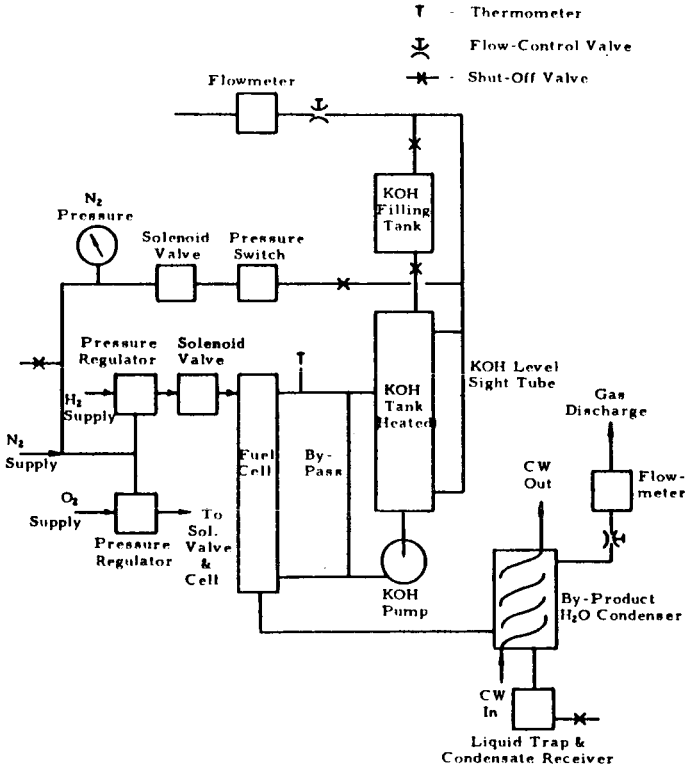

D-3124

Fig. 6 - NASA Pressure Cell Test Scheme.

In addition, a second tank (4) was installed above the main reservoir. This can be isolated from the system by means of valves above and below, and provides a means for adding electrolyte to the pressurized system, if desired. Both of these tanks are provided with service openings (normally plugged). When reference electrode readings are required, the electrode (a Zn wire) is inserted directly into the main KOH reservoir.

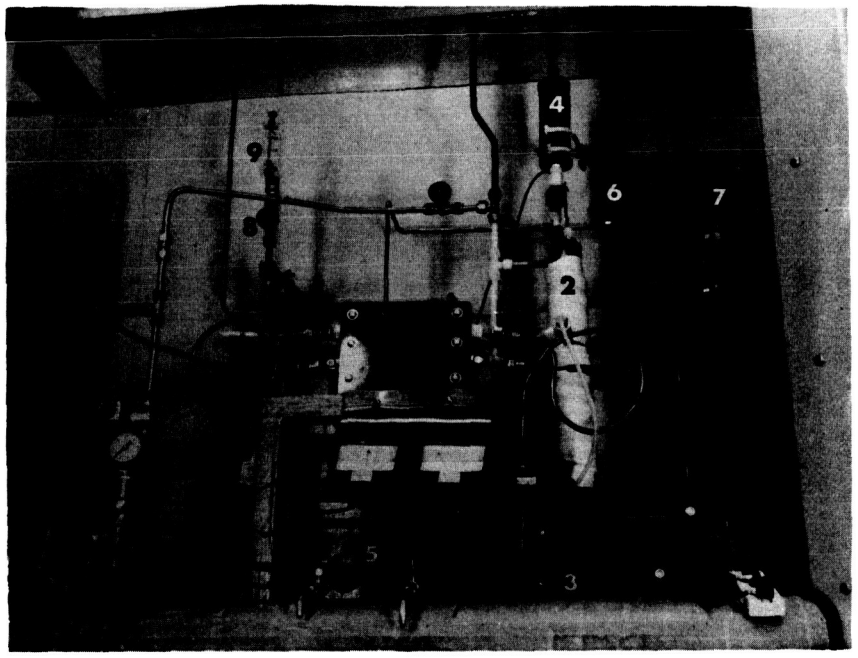

D-3118

Fig. 7 - NASA Pressure Cell Test Scheme.

Each exit gas passes through a condenser and trap (5)—stainless steel— in a manner similar to that already described. The flow rate is adjusted by means of a control valve (6), and measured by a flow meter (7) at the discharge end of the line. A continuous purge of nitrogen is also maintained through valve (8) and flow meter (9) which prevents the accumulation of hydrogen and oxygen above the electrolyte.

Safety features were provided to completely shut down the system, in the event of loss of nitrogen pressure or drop in electrolyte level, by means of a pressure switch in the nitrogen line, solenoid valves in all of the gas lines, and a probe in the electrolyte reservoir.

Six additional test facilities are in use, primarily for life testing of single cells. These have been somewhat more elaborately instrumented. Figures 8 and 9 show the schematic and photograph of this facility. Identifying numbers in Fig. 9 are as follows: (1) fuel cell; (2) heated electrolyte reservoir; (3) instrument panel containing pressure regulators, flowmeters, gages, voltmeter, and ammeter; (4) condenser (exit gas line), and (5) condensate receiver.

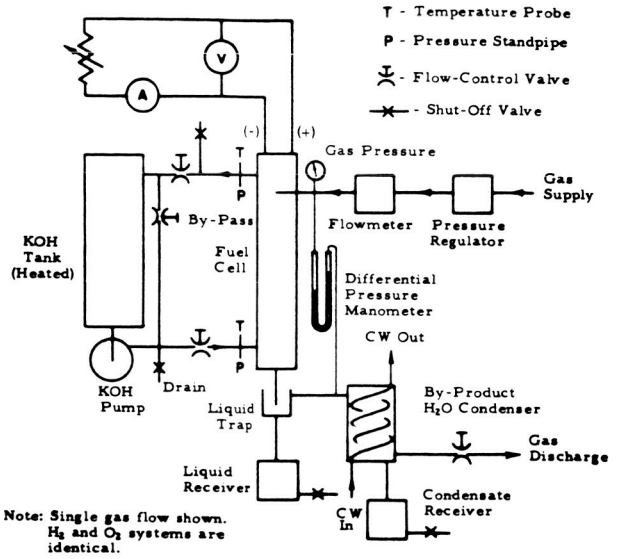

D-3123

Fig. 8 - NASA Single Cell Test, Scheme B.

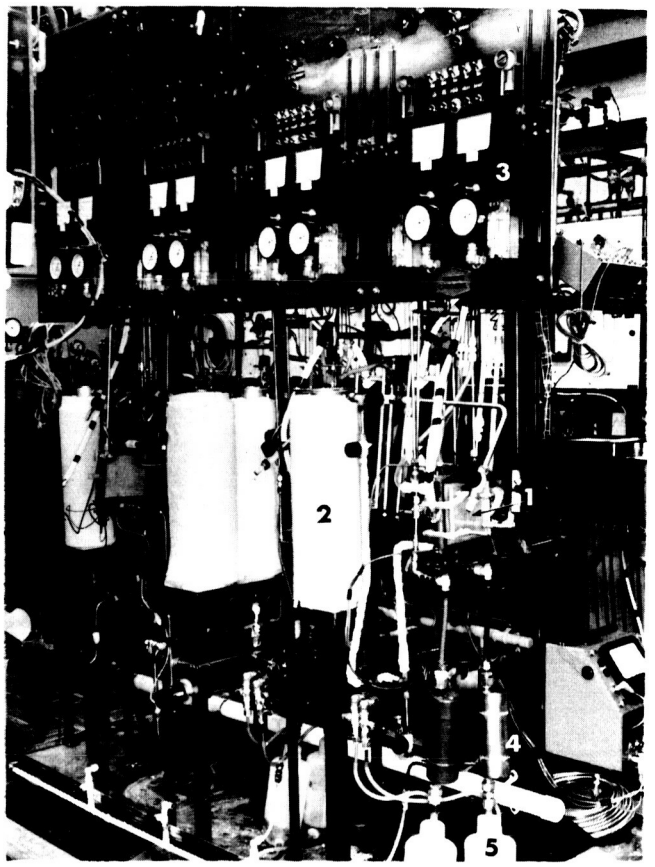

D-3120

Fig. 9 - NASA Single Cell Test, Scheme B.

D. Experimental Results.

1. Summary of Large Cell Data.

The bulk of the testing to date has been done with 4" x 4-1/2" (0.125 ft.^{2}) cells. Table I lists the cells which have been built and (with the exception of a few) tested to date. The electrode types, additional current collectors, and electrolyte separators are designated by numbers described in the footnotes following the table. The term "additional current collectors" refers to a metal member in addition to the porous metal or screen which forms an integral part of the electrode.

In the case of electrodes made with precatalyzed carbon, the catalyst levels are rather approximate since there was some variation in electrode thickness, and the values were not calculated for each individual electrode.

Table II summarizes all of the cell data obtained at a current density of 200 ASF. In some cases cells were operated for additional periods at lower current densities, but these data are not included here. Likewise, cells which were operated at current densities other than 200 ASF are omitted. Both terminal and IR-free voltage data were obtained. The latter values were measured by means of a Kordesch-Marko bridge—widely used for this type of measurement.

Table III presents IR-free cathode and anode data (versus a zinc wire reference electrode). For convenience, these data are listed according to electrode type rather than consecutively.

The voltage data in Tables II and III are listed as "initial," "peak," and "final". Initial values were usually taken on the first test day; final values refer to the last ones taken before the test was terminated (or the load reduced)—usually on the last test day. Peak values refer to the "best" values measured during the test period. Cell, anode, and cathode peak values do not, of course, necessarily fall on the same test day.

The electrode performance goal of 900 mv terminal voltage with 20 mv or less voltage degradation tolerable over a 500-hour period at 200 ASF, in effect, establishes a "cut-off" voltage of 880 mv as a minimum acceptable value. Of the cells tabulated in Table II, only Cell A-015 has remained above 880 mv for over 500 hours; this cell is operating above 880 mv after more than 800 hours, with the test still in progress. Many of the tests, in particular all of those employing Type-2 cathodes, were conducted for the purpose of obtaining specific experimental infor-

TABLE I

CELL DESCRIPTIONS

Cell No.	Electrode Types	Catalyst Level (mg/cm^2)	Additional Current-Collector Types	Electrolyte-Separator Types
A-001	2-1 Cathode	1.0	1	1
	2-1 Anode	2.5	1	
A-002	2-2 Cathode	8.0	None	1
	2-2 Anode	8.0	None	
A-003	2-2 Cathode	8.0	2	1
	2-2 Anode	8.0	2	
A-004	2-1 Cathode	1.0	1	2
	2-1 Anode	2.5	1	
A-005	2-3 Cathode	~5.0	3	2
	2-3 Anode	~5.0	3	
A-006	LAB-40 Cathode	40.0	3	2
	LAB-40 Anode	40.0	3	
A-007	3-1 Cathode	4.0	3	2
	2-1 Anode	2.5	3	
A-008	5-1 Cathode	1.0	2	2
	2-1 Anode	2.5	2	
A-009	2-1 Cathode	1.0	2	2
	2-1 Anode	2.5	2	
A-010	2-1 Cathode	1.0	2	3
	2-1 Anode	2.5	2	
A-011	2-3 Cathode	~5.0	2	4
	Modified AB-40 Anode	40.0	2	
A-012	4-1 Cathode	1.0	4	4
	2-1 Anode	2.5	2	
A-013	LAB-40 Cathode	40.0	2	2
	LAB-40 Anode	40.0	2	
A-014	LAB-40 Cathode	40.0	3	2
	LAB-40 Anode	40.0	3	
A-015	LAB-40 Cathode	40.0	2	2
	LAB-40 Anode	40.0	2	
A-016	2-3 Cathode	~5.0	3	2
	2-1 Anode	2.5	2	
A-017	5-3 Cathode	~5.0	3	2
	2-1 Anode	2.5	2	
A-018	LAB-40 Cathode	40.0	3	2
	LAB-40 Anode	40.0	3	

(Continued)

TABLE I

(Continued)

Cell No.	Electrode Types	Catalyst Level (mg/cm^2)	Additional Current-Collector Types	Electrolyte-Separator Types
A-019	LAB-40 Cathode	40.0	2	2
	LAB-40 Anode	40.0	2	
A-020	LAB-40 Cathode	40.0	2	2
	LAB-40 Anode	40.0	2	
A-021	LAB-40 Cathode	40.0	2	2
	LAB-40 Anode	40.0	2	
A-022	LAB-40 Cathode	40.0	2	2
	LAB-40 Anode	40.0	2	
A-023	LAB-40 Cathode	40.0	2	2
	LAB-40 Anode	40.0	2	
A-024	2-4 Cathode	~10.0	None	2
	2-1 Anode	2.5	2	
A-025	2-4 Cathode	~10.0	None	2
	2-1 Anode	2.5	2	
A-026	5-4 Cathode	~10.0	2	2
	2-1 Anode	2.5	2	
A-027	5-4 Cathode	~10.0	2	2
	2-1 Anode	2.5	2	
A-028	LAB-40 Cathode	40.0	2	2
	LAB-40 Anode	40.0	2	
A-029	5-4 Cathode	~10.0	2	2
	2-1 Anode	2.5	2	
A-030	4-2 Cathode	2.0	4	2
	2-1 Anode	2.5	2	
A-031	LAB-40 Cathode	40.0	2	2
	LAB-40 Anode	40.0	2	
A-032	5-4 Cathode	~10.0	2	2
	2-1 Anode	2.5	2	
A-033	H9454N Cathode	9.0	3	2
	H9454N Anode	9.0	3	
A-034	5-4 Cathode	~10.0	3	2
	2-1 Anode	2.5	3	
A-035	H9454N Cathode	9.0	3	2
	2-1 Anode	2.5	3	
A-036	LAB-40 Cathode	40.0	2	2
	LAB-40 Anode	40.0	2	

(See Legend Notes on following page)

TABLE I NOTES

Electrode Types:

2-1	C on porous Ni; post-catalyzed
2-2	C on porous Ag; post-catalyzed
2-3	C on porous Ni; precatalyzed
2-4	C on porous Ag; precatalyzed
3-1	C on porous Ni (modified structure); post-catalyzed
4-1	C on porous Teflon; post-catalyzed
4-2	C on porous Teflon; precatalyzed
5-1	C on Ni screen + Teflon backing; post-catalyzed
5-3	C on Ni screen + Teflon backing; precatalyzed
5-4	C on Ag screen + Teflon backing; precatalyzed
LAB-40	Cyanamid
H9454N	ChemCell

Additional Current Collector Types:

1	Pressure contact; Ag screens between electrode and Ni collector plate
2	Silver frame and tab
3	Same as 2, plus Ag screen pressed against face
4	Pressure contact; screen pressed against electrode face and extended as collector tab

Electrolyte Separator Types:

1	Lamports Style No. 7700 polypropylene mesh
2	Exmet, Code-10 expanded Nylon, 25-1 (stabilized)
3	Webril SM91 oriented fiber, polypropylene
4	Exmet, expanded polypropylene, 25-1

TABLE II

SUMMARY OF CELL DATA AT 200 ASF, 15 PSIA

Cell No.	Temp. (°C)	Cell Voltage (IR-Free) Initial	Peak	Final	Cell Voltage (IR-Inc) Initial	Peak	Final	Hours on Test	Reason for Termination of Test
A-001	91-105	0.856	-----	0.842	0.770	-----	0.706	29	Large increase in IR drop.
A-002	98-102	0.891	0.891	0.036	0.827	0.827	-----	68	Cathode failure.
A-003	97-103	0.888	0.896	0.770	0.836	0.836	-----	31	Poor cathode.
A-004	98-102	0.856	0.886	0.863	0.756	0.756	0.638	51	Large increase in IR drop.
A-005	98	0.801	--- -	-----	0.718	-----	-----	---	Poor anode.
A-006	95-102	0.936	0.949	0.886	0.884	0.894	0.828	~263	Cathode weeping.
A-009	97-101	0.866	0.871	0.851	0.786	0.786	0.726	78	Large increase in IR drop.
A-010	97	0.885	-----	0.892	0.762	-----	0.696	30	Large increase in IR drop.
A-013	105-111	0.921	0.932	0.858	0.868	0.868	0.800	97	Frame leakage.
A-014	86-93	0.940	0.950	0.950	0.880	0.888	0.888	~77	Cell damaged during lab power shutdown.
A-015	See Figures 14 and 18. (Life Test Cell)							800	Still on test.
A-016	98-102	0.879	0.925	0.643	0.800	0.800	0.466	~83	Cathode weeping; both electrodes poor.
A-017	83-93	0.913	0.913	0.723	0.844	0.844	0.634	34	Cathode weeping; both electrodes poor.
A-018	See Figures 15 and 19 (Life Test Cell)							800	Performance dropped.
A-019	87-92	0.921	0.921	0.790	0.884	0.862	0.760	363	Poor anode.
A-023	89-91	0.900	-----	-----	0.865	-----	-----	---	Electrolyte leakage; defective cell.
A-024	~85	0.882	-----	-----	0.806	-----	-----	~18	Cathode completely wet.
A-026	88-95	0.892	0.922	0.889	0.802	0.842	0.790	53	Cathode weeping.
A-027	85-93	0.907	0.904	0.762	0.814	0.814	0.664	476	Cathode weeping; both electrodes poor.
A-029	85-94	0.893	0.893	0.800	0.806	0.818	0.665	281	Cathode weeping; poor anode.
A-030	89-91	0.850	-----	0.633	0.706	-----	0.500	18	Poor cathode.
A-036	85-89	0.932			0.895				New cell; still on test.

TABLE III

SUMMARY OF ELECTRODE DATA - 200 ASF, 15 PSIA
(IR-Free Potentials vs. Zinc Reference Electrodes)

Type	Cell No.	Initial	Peak	Final
		Cathode Data		
2-1	A-004	1.377	1.392	1.372
	A-009	1.371	1.388	1.376
	A-010	1.394	1.409	1.409
2-2	A-002	-----	1.382	0.668
	A-003	-----	1.393	1.249
2-3 & 2-4	A-005	-----	1.487	-----
	A-016	1.368	1.415	1.193
	A-024	1.361	-----	-----
4-2	A-030	1.347	-----	1.147
5-3 & 5-4	A-017	1.405	1.405	1.310
	A-026	1.384	1.413	1.370
	A-027	1.399	1.405	1.318
	A-029	1.375	1.410	1.390
LAB-40	A-006	-----	1.436	1.376
	A-013	1.420	1.465	1.364
	A-014	1.433	1.439	1.439
	A-019	1.397	1.410	1.385
	A-023	1.390	-----	-----
	A-031	1.401	-----	-----
	A-036	1.455	-----	-----
		Anode Data		
2-1	A-004	0.523	0.507	0.513
	A-009	0.508	0.508	0.532
	A-010	0.513	0.513	0.522
	A-016	0.488	0.488	0.558
	A-017	0.492	0.492	0.591
	A-024	0.481	-----	-----
	A-027	0.492	0.492	0.558
	A-029	0.482	0.482	0.590
	A-030	0.499	0.499	0.517
2-2	A-002	-----	0.528	0.630
	A-003	-----	0.499	0.478
2-3	A-005	-----	-----	0.685
LAB-40	A-006	-----	0.487	0.491
	A-013	0.500	0.500	0.508
	A-014	0.491	0.491	0.492
	A-019	0.479	0.479	0.600
	A-023	0.487	-----	-----
	A-031	0.481	-----	-----
	A-036	0.525	-----	-----

mation such as the effect of current collector type, choice of separator, method of catalysis, etc. As a result, most of the tests shown in Table II were deliberately terminated when the desired information was obtained. Only two cell tests to date (Cells A-015 and A-018) have been conducted on the life-test racks of the main testing facility, the remaining tests being conducted on the experimental test racks of the research facility. Life test data on cells A-015 and A-018 will be detailed later (in 3. Cell Life).

A low terminal voltage for a cell can imply excessive polarization, high internal resistance within the cell, high current collector losses, or more usually, some combination of these factors. Comparison of the IR-free potentials and terminal voltages shown in Table II indicates that an IR drop of 50 mv or less can be realized at 200 ASF. To obtain a net 900 mv at the cell terminals thus requires a difference in electrode potential of 950 mv at 200 ASF. The highest IR-free differences in potential observed thus far, including all values above 900 mv, are listed in Table IV.

TABLE IV

CELLS WITH HIGHEST IR-FREE POTENTIALS (200 ASF, 15 PSIA)

Cell No.	Type	IR-Free Potentials
A-014	LAB-40 Cathode LAB-40 Anode	0.950v
A-006	LAB-40 Cathode LAB-40 Anode	0.949v
A-013	LAB-40 Cathode LAB-40 Anode	0.932v
A-016	2-3 Cathode 2-1 Anode	0.925v
A-026	5-4 Cathode 2-1 Anode	0.922v
A-019	LAB-40 Cathode LAB-40 Anode	0.921v
A-017	5-3 Cathode 2-1 Anode	0.913v
A-027	5-4 Cathode 2-1 Anode	0.907v

The best terminal voltages obtained to date (0.88, or better) were for cells A-006, and A-014, both with LAB-40 electrodes. On the basis of these encouraging results, replicate cells A-015 and A-018 were placed on life test.

2. Catalyst Loading.

One of the original objectives of this program was to improve the potentials of fuel cell electrodes by increasing the content and effectiveness of the noble metal which serves as electrocatalyst. Evaluations have been carried out both in small (2.0 cm^2) cells as well as 4" x 4-1/2" cells, so that a discussion of this subject will include data of the former type as well as that presented in the tables of the preceding section.

In small-cell testing, both pre- and post-catalysis of cathodes has been carried out. A series of Type-5 cathodes, post-catalyzed at the 1, 5, and 10 mg/cm^2 levels and tested over a 3-day period, showed the 1 mg/cm^2 loading to be poor. The 5 mg/cm^2 loading was found to be slightly better than the 10 mg/cm^2, both of which were far superior to the 1 mg/cm^2 electrodes (see Table V).

TABLE V

POST-CATALYSIS OF TYPE-5 CATHODES

12 M KOH; ~80°C; 200 ASF; 3-Day Test Duration, 15 psia

Catalyst Loading	IR-Free Potentials vs. Zinc Ref. (Volts) Initial	Peak	Final
1 mg/cm^2 (2 tests)	1.314	1.314	1.224
	1.326	1.326	1.279
5 mg/cm^2 (3 tests)	1.334	1.405	1.405
	1.343	1.402	1.364
	1.344	1.400	1.400
10 mg/cm^2 (3 tests)	1.321	1.397	1.397
	1.324	1.390	1.384
	1.318	1.380	1.378

Small-cell tests of precatalyzed cathodes have been conducted at 200 ASF. Cathodes catalyzed at approximately the 10 mg/cm^2 level have been tested over a two-week period with encouraging results. These were of Type-5 except for omission of the Teflon backing (see Table VI).

TABLE VI

PRECATALYSIS OF TYPE-5 CATHODES*

12 M KOH; ~80°C; 200 ASF; 2-Week Test Duration, 15 psia

Catalyst Loading ~10 mg/cm^2	IR-Free Potentials vs. Zinc Ref. (Volts) Initial	Peak	Final
4 Cells Tested	1.424	1.424	1.422
	1.425	1.425	1.415
	1.416	1.416	1.390
	1.405	1.415	1.404

* Teflon backing omitted.

Data obtained with large-cell tests, as summarized in Table III, have also shown favorable initial performance with precatalyzed cathodes (Types 5-3, and 5-4). The peak values of these cathodes corresponded fairly well with those obtained with the small cells (Table VI). The rate of potential degradation of the cathode was far higher in 4" x 4-1/2" cells A-017, A-026, A-027, and A-029 (all employing precatalyzed Type-5 cathodes) than for the small test cells listed in Table VI. The cathodes of Cells A-017, A-026, A-027, and A-029 show a potential degradation of 280, 26, 17, and 7 mv/100 hours, respectively, compared with less than 3 mv/100 hours for the cathodes of Table VI. The difference is possibly related to the Teflon backing (present in the large-cell cathodes but absent in those used in the small cells). The overall desirability of this backing is questionable at present, and will be discussed later.

Post-catalyzed Type 2-1 cathodes gave peak IR-free potentials at 200 ASF which averaged only slightly lower than the precatalyzed Type-5. The Type-2 cathodes, however, showed a serious resistance problem which will also be discussed later, and which makes these look unsuitable at present.

In general, the best overall cathode performance at 200 ASF and 90-100°C has been achieved by the American Cyanamid LAB-40 electrodes (Table III) which consist of 40 mg Pt/cm^2, Teflon-bonded to a heavy gold-plated nickel screen, and backed with porous Teflon.

Catalysis experiments with anodes have been unrewarding. Earlier work done prior to this contract showed rather conclusively that post-catalysis of Type-2 anodes above the level of a few milligrams/cm^2 did not improve their potentials, and that too much catalyst was even detrimental. Precatalyzed anodes (5 - 10 mg/cm^2 range) have been particularly disappointing, and Type-5 anodes (either pre- or post-catalyzed) have so far been entirely unsuccessful. The failure of the latter type is related to both an over-repellent electrode surface (post-catalyzed anodes), and the inability at present to make precatalyzed anodes of suitable mechanical strength. Furthermore, the precatalyzed carbon, even when used in Type-2 anodes, has not looked very promising from an anode-potential standpoint at 200 ASF.

LAB-40 anodes have been variable in performance. By referring to Table III data from seven test cells can be examined. Cell A-006, for example, contained an anode which performed outstandingly. On the other hand, Cell A-019, although showing good initial anode performance, suffered irreversibly merely by taking it off

load, shutting off the hydrogen supply, and turning off the heat over one weekend. The spread of the anode data is too broad to permit any final conclusions at this time. Type 2-1 anodes and LAB-40 anodes show comparable initial potentials at 200 ASF (Table III). The LAB-40 anodes under ideal operating conditions show less voltage degradation than the Type 2-1 anodes tested to date, but the former are quite sensitive to abuse. A simple test interruption, permitting the cell to cool to room temperature, can cause irreversible damage. Preliminary indications are that the problem area is delamination of the layer structure under thermal cycling stress. Analysis of performance data for Type 2-1 anodes is clouded by the fact that every cell incorporating such an anode employed also a carbon cathode (of Type-2, 3, 4, or 5); see Table I. A majority of these test cells incorporated Type-2 cathodes, which have since been shown to be unstable under conditions of 100°C operation. Corrosive degradation of the cathode is known to be capable of damaging the anode, presumably through deposition of degradation products upon the anode catalyst. To examine this possibility, cells employing Type 2-1 anodes with LAB-40 cathodes will be placed on test; any major improvement in anode stability in such a cell will lend credence to the hypothesis of cathode-anode interactions in previously tested cells.

3. Cell Life.

In addition to the data presented in Table II, the life histories of several cells are presented in Figs. 10 through 14.

Figures 10 and 11 show data for cells with Type 5-4 cathodes and 2-1 anodes, and can be compared directly with the 200 ASF data of a LAB-40 cell (A-014) shown in Fig. 12. The latter shows a peak terminal voltage of almost 0.89 volt after three days on test. Cells A-027 and A-029, on the other hand, have peak terminal voltages of only 0.82 volt. The difference between these two types of cells can be seen to be in both the cathode potentials and the IR drops. In all cells the IR drops are seen to have remained quite constant, indicating satisfactory bonding of the electrode materials to their conductor supports. Type-5 cathode failures have invariably been associated with "weeping" of electrolyte through the electrode structure. Type-2 anode degradation is usually not accompanied by visible wetting through to the back of the electrode.

Cyanamid Cell No. A-014 (Fig. 12) had an interesting history which helps pinpoint one of the weaknesses of this type of electrode. After three days on test the cell was shut down. Upon reactivation it was found to be very poor. Although

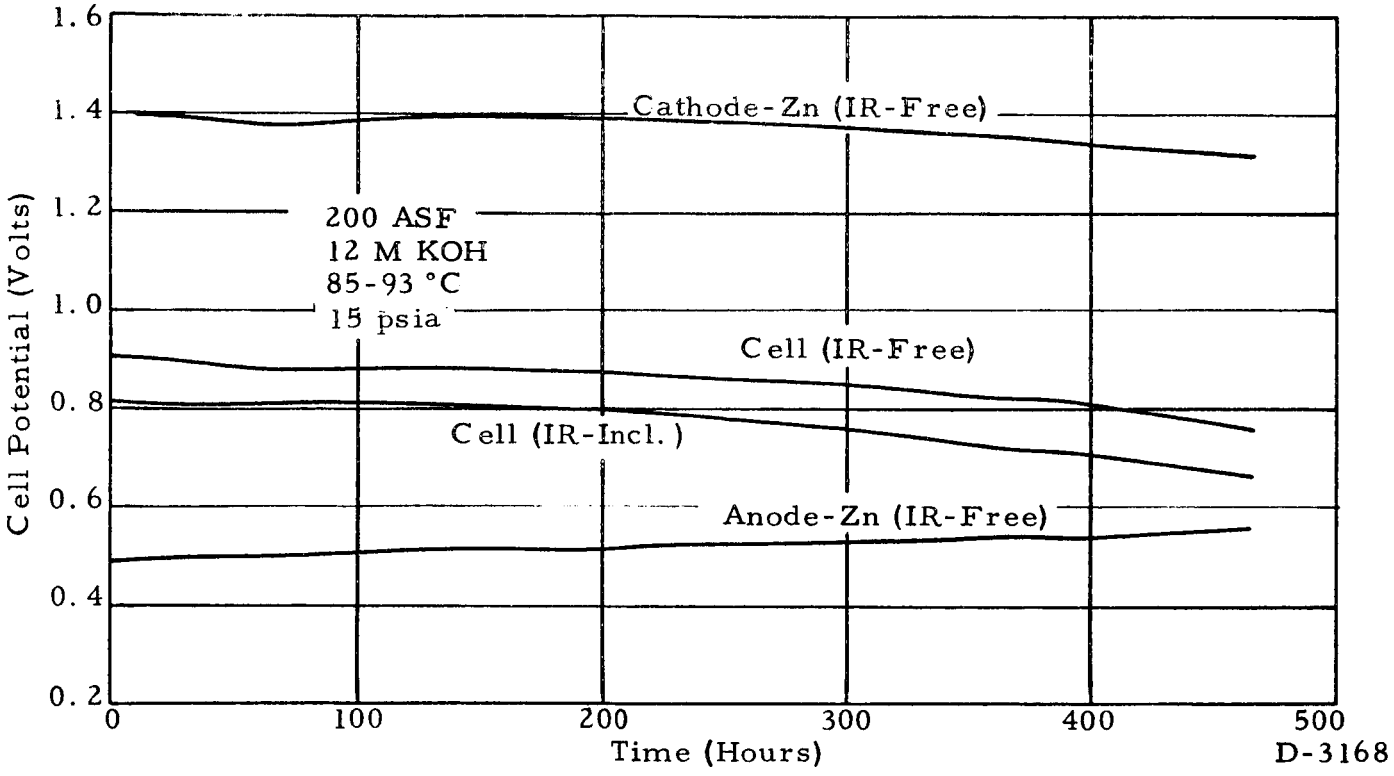

Fig. 10 - Life History, Cell No. A-027.

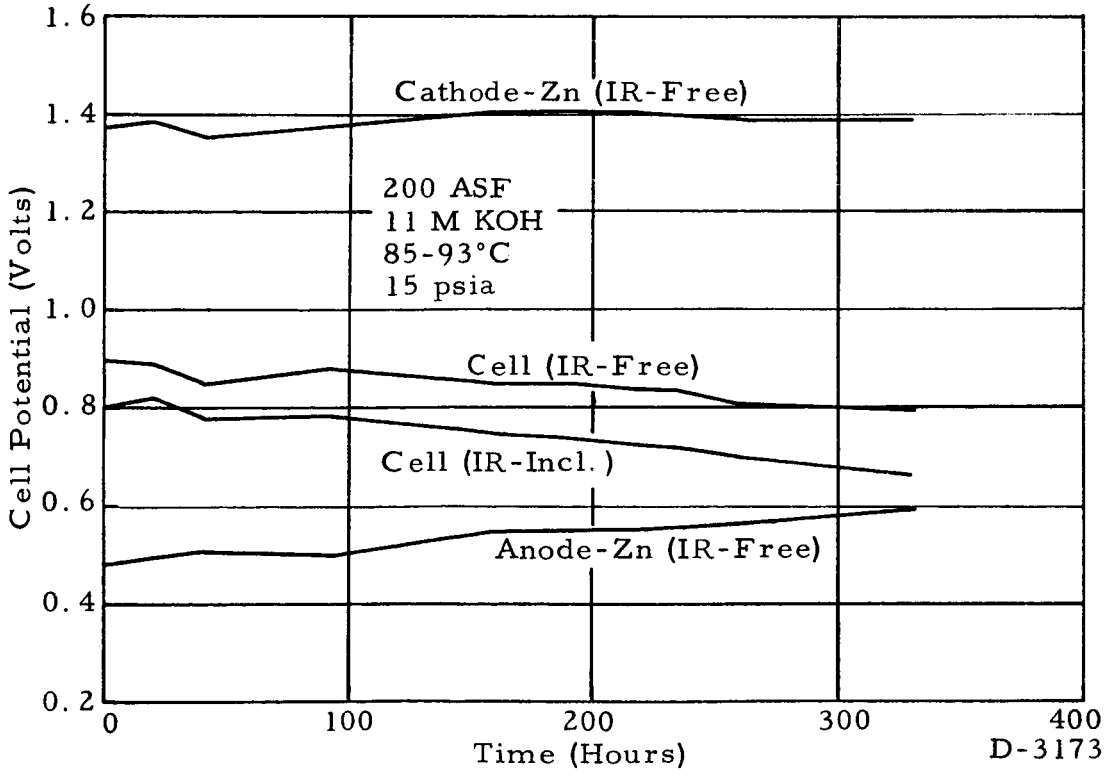

Fig. 11 - Life History, Cell No. A-029.

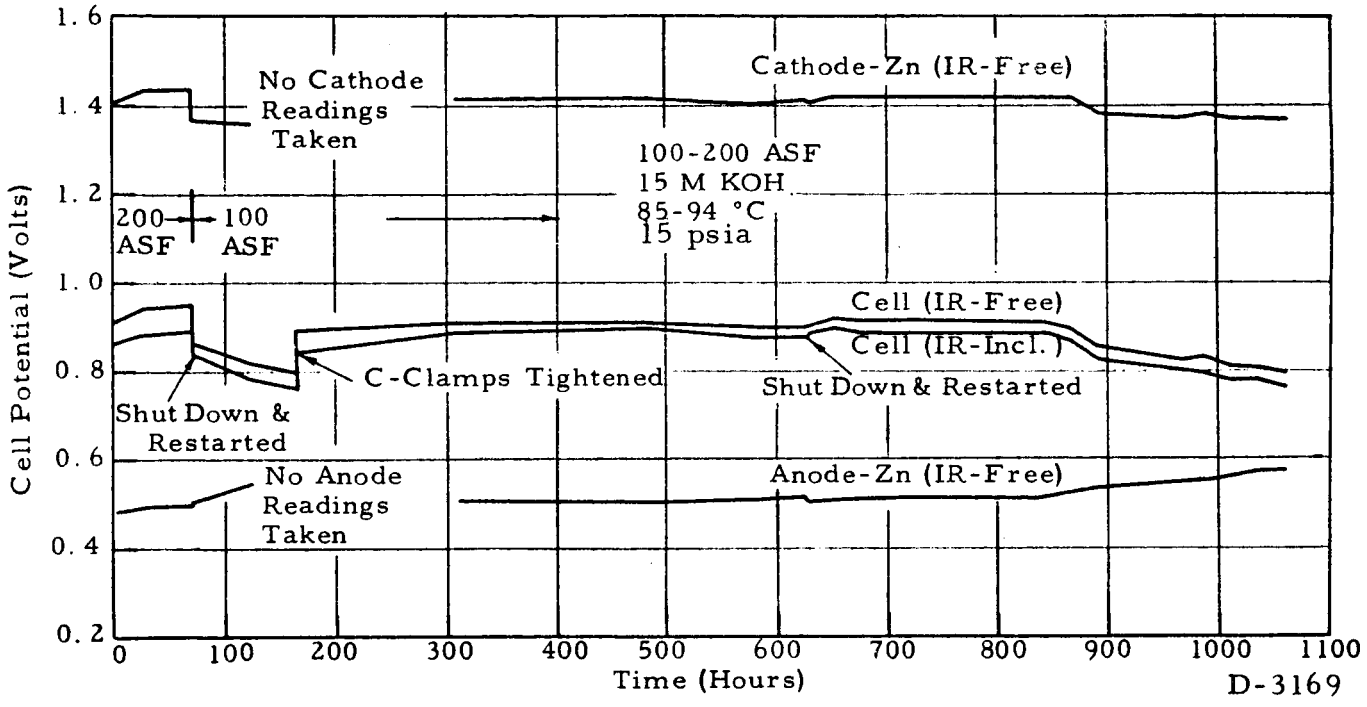

Fig. 12 - Life History, Cell No. A-014.

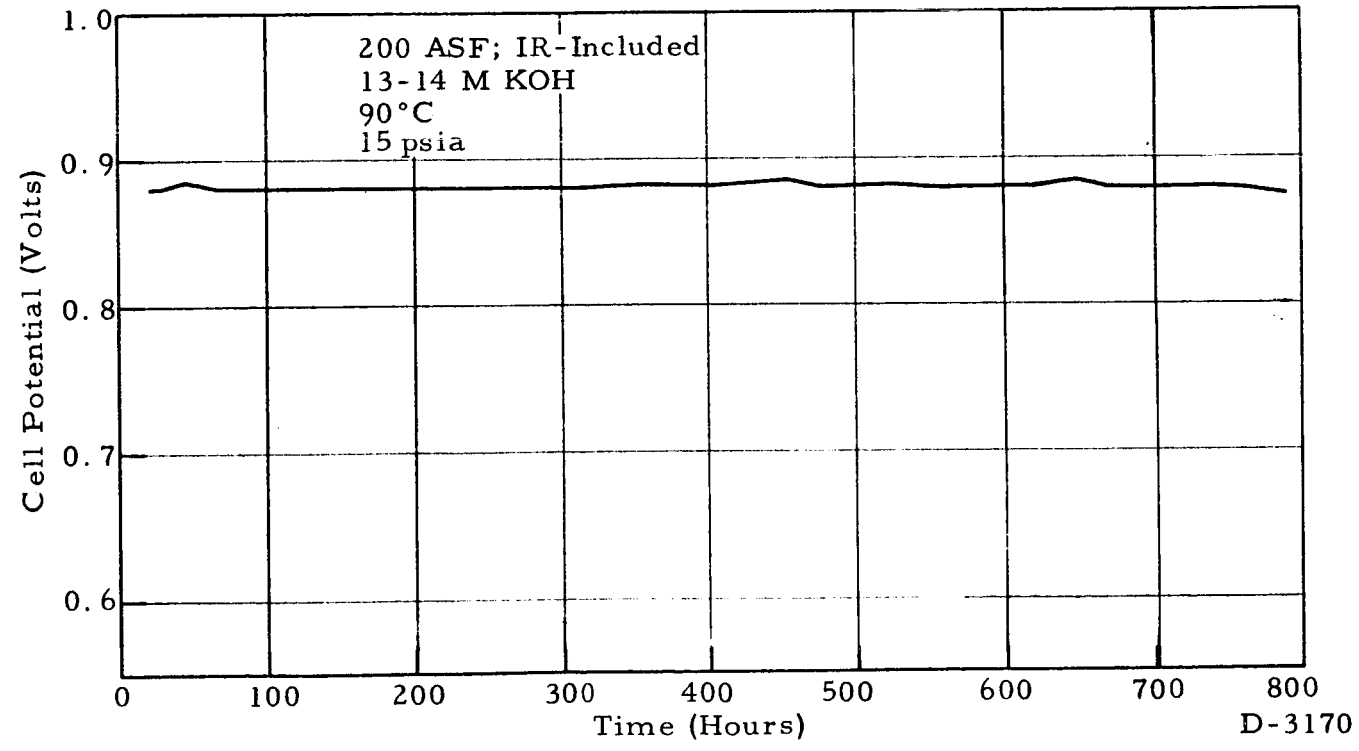

Fig. 13 - Life History, Cell No. A-015.

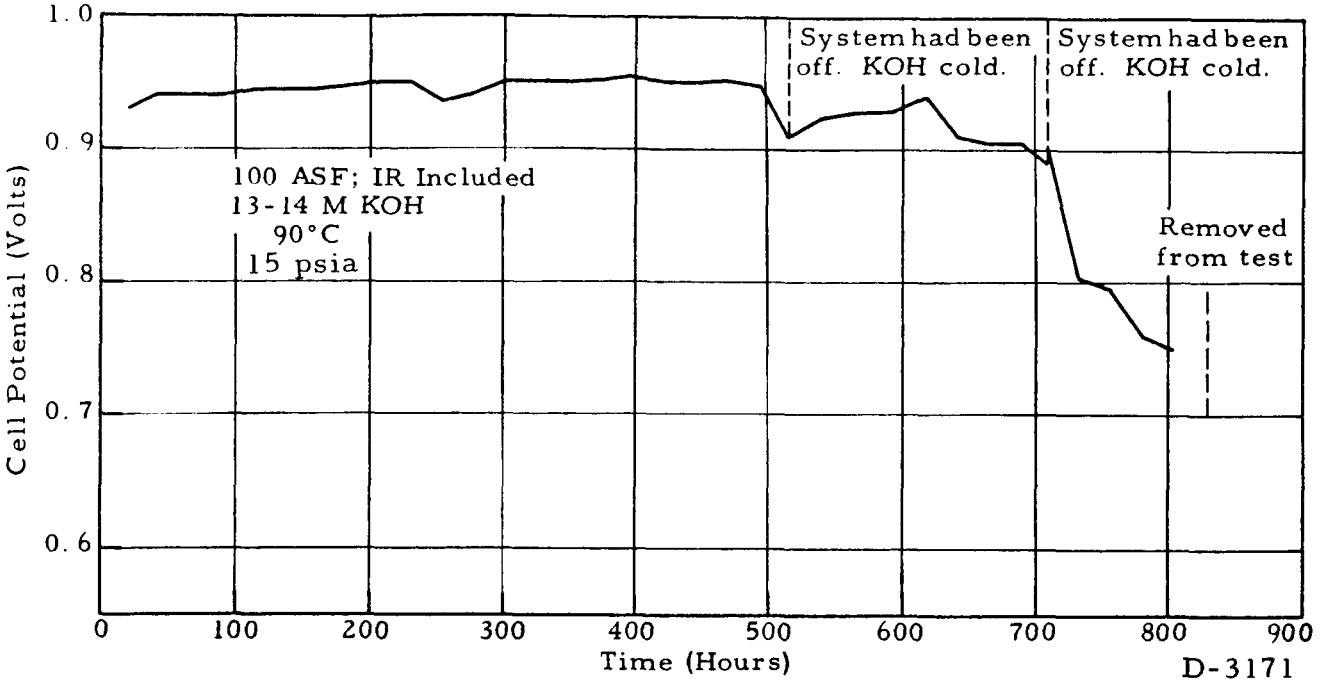

Fig. 14 - Life History, Cell No. A-018.

from the start this cell had been supported by auxiliary C-clamps, these were found to be rather loose, and on the 7th day were tightened. The voltage improvement was dramatic—about 100 mv. Since the magnitude of improvement was the same for both IR-free and IR-included readings, it was concluded that the Teflon backing had loosened because of the shutdown procedure, and electrolyte had accumulated in the pockets between the Teflon and the electrode proper.

Figures 13 and 14 are two of the most recent life tests obtained with LAB-40 cells; one at 200 ASF, and one at 100 ASF. These represent the best life data obtained so far. The large changes in cell voltage near 500 hours and after 700 hours for cell A-018 (Fig. 14) are associated with thermal cycling during test shutdowns. The fact that cell A-015 has shown better voltage stability at 200 ASF than cell A-018 at 100 ASF suggests that the current density during operation is not the primary factor influencing operating life.

4. Current-Voltage Relationships.

Current-voltage data obtained for the cells discussed in the preceding sections are presented in Figs. 15 through 18. Figure 15 shows curves obtained with the two cells with Type 5-4 cathodes and Type 2-1 anodes, representing data taken on the first day of operation, and is therefore an indication of maximum performance

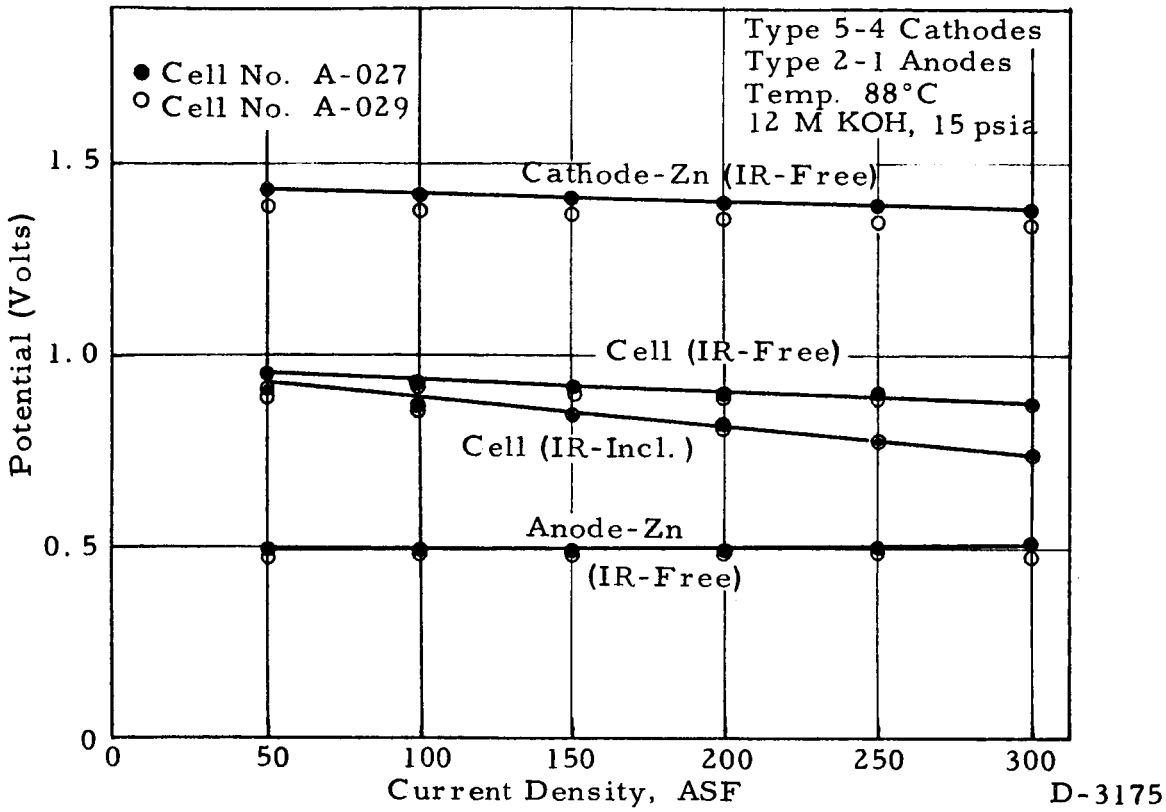

Fig. 15 - Current-Voltage Data for Cell Nos. A-027 and A-029.

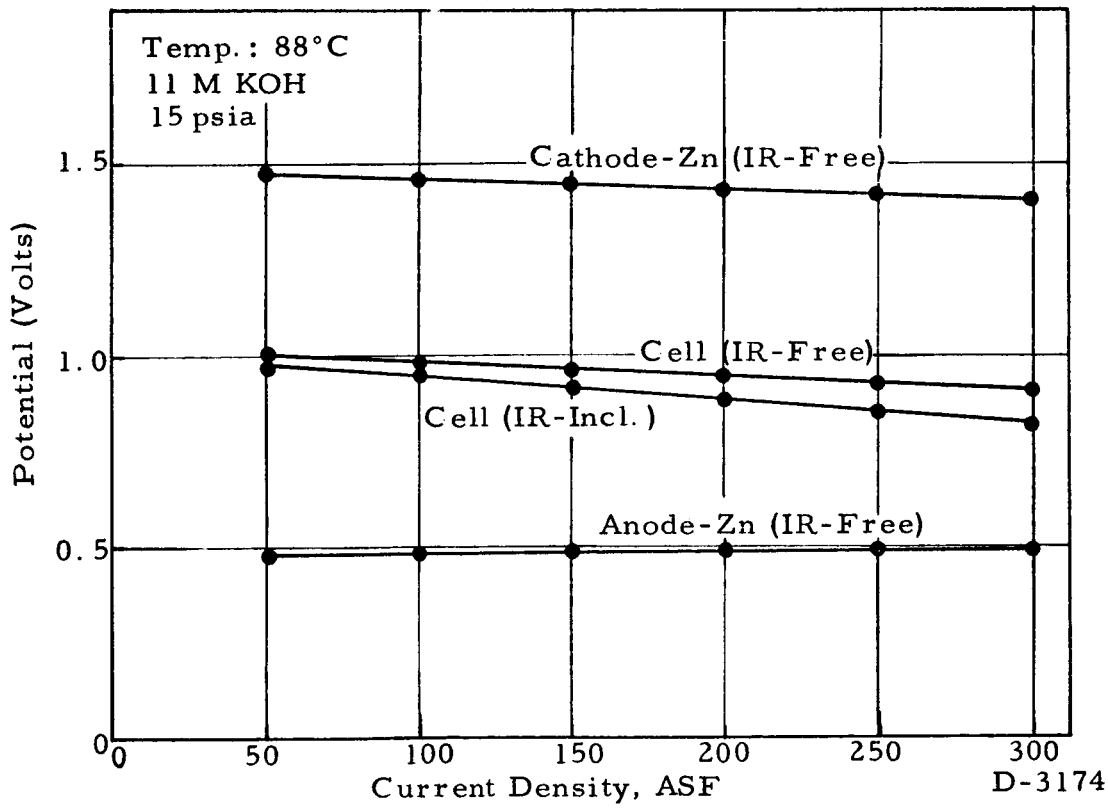

Fig. 16 - Current-Voltage Data for Cell No. A-014.

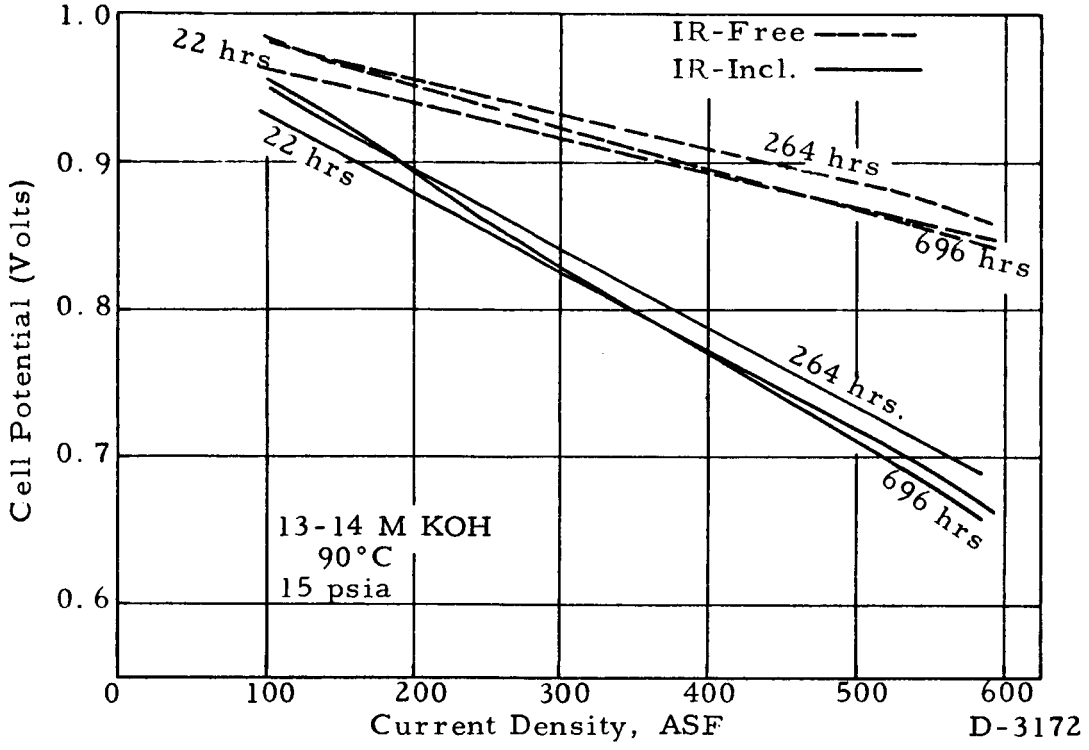

Fig. 17 - Current-Voltage Data for Cell No. A-015.

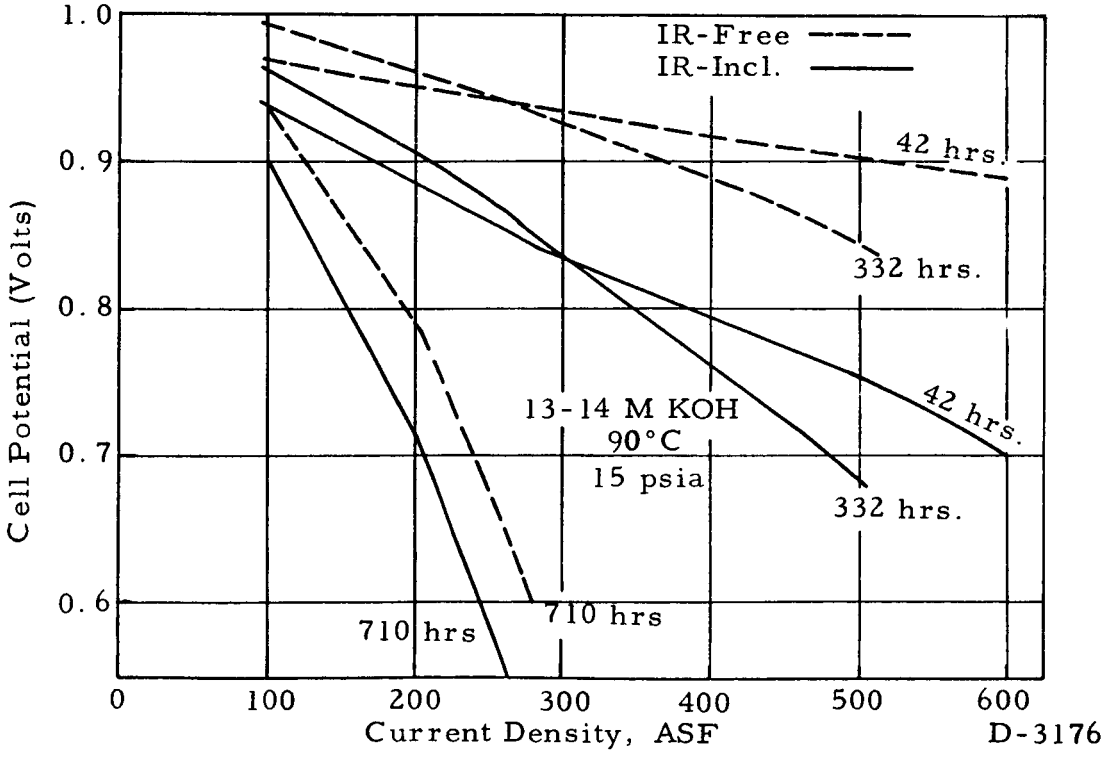

Fig. 18 - Current-Voltage Data for Cell No. A-018

achievable with these types of electrodes. Although cathode potentials show some improvement during the first few days (6 mv at 200 ASF for Cell A-027; 35 mv for Cell A-029), anode potentials showed degradation during the same period, with the result that the initial cell voltages were at a maximum on the first test day.

Comparison of these data with those for LAB-40 Cell No. A-014 (Fig. 16), which also represent initial test data, shows that in spite of their somewhat lower cathode potentials, the Type-5 IR-free cathode curves were slightly flatter than the LAB-40. The corresponding anode curves were almost identical.

Figures 17 and 18 show current-voltage curves taken periodically during life testing of Cells A-015 and A-018 (LAB-40 anodes and cathode). Figure 17 shows that the internal resistance of Cell A-015 has remained constant within experimental error over the test period. The change in IR drop shown for Cell A-018 in Fig. 18 indicates a slight increase in internal resistance, from about 2.4 milliohms at 42 hours life to about 2.9 milliohms at 710 hours of life. The total degradation in terminal voltage of the cell at 200 ASF between 42 hours and 710 hours was 172 mv. The 0.5 milliohm increase in internal resistance of the cell can account for a 12 mv loss at 25 amperes (200 ASF times 1/8 ft^2 cell area), leaving 160 mv to be accounted for as an increase in electrode polarization. This same value can be arrived at more directly by reading the difference in IR-free potentials plotted in Fig. 18. These observations are consistent with the previously presented hypothesis that delamination of the LAB-40 electrode at the porous Teflon-active layer interface, followed by flooding of the resulting gap, can block gas access to the catalyst and lead to high polarization losses.

5. Effects of Temperature and Pressure.

In attempting to improve the level of cell performance, the effects of temperature and pressure have been studied to a limited extent. Both of these parameters have a significant effect which will require further investigation.

Figure 19 shows how cell temperature and electrolyte concentration are interrelated, as demonstrated by (LAB-40) Cell No. A-013. At each electrolyte concentration, the cell voltage was observed to increase with increasing temperature until a maximum was reached, after which it decreased. Furthermore, with increasing concentrations, this maximum was seen to shift to the right, increasing from about 100°C with 11.6 M KOH to 120°C with 14.8 M KOH.

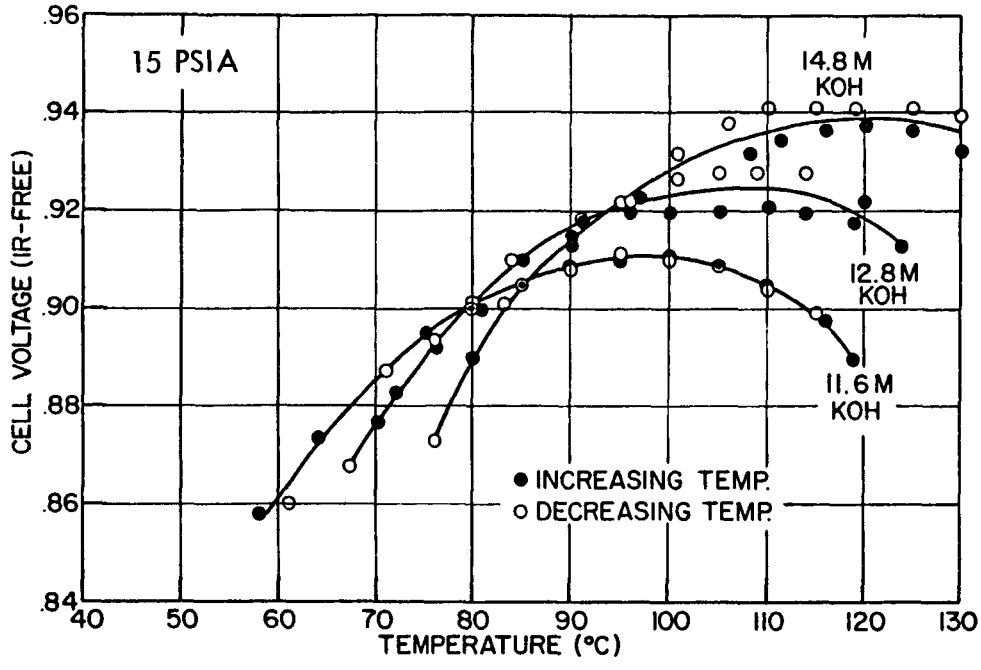

D-3062

Fig. 19 - Temperature-Electrolyte Concentration Effects (Cell Nr. A-013).

The maximum IR-free cell voltages at these two points were 0. 911 and 0. 939 volt, respectively. Tests have not been made to correlate these conditions with cell life, however, earlier experience has indicated generally shorter lives at excessive temperature. For most of our testing, a temperature in the vicinity of 90°C has been selected, since at this point the cell voltage is rather insensitive to electrolyte concentration as can be seen by inspection of Fig. 19. However, the possible beneficial effects of increasing both cell temperature and KOH molarity must not be overlooked

An additional 30 mv appears to be obtainable by pressurizing the system (both electrolyte and gases) to 15 psig. Figures 20 and 21 show the effect obtained on another LAB-40 cell (No. A-031) at pressures up to 45 psig. It can be observed that the improvement obtained by pressurization from atmospheric pressure to 15 psig is relatively large as compared to the additional gain obtained by going to still higher pressures.

From these data, both increasing the pressure to 15 psig and the temperature to 130°C (with a KOH concentration of 14-15 M) would add 50 - 60 mv to the cell voltage at 200 ASF and bring it up to 0. 93-0. 95 volt terminal.

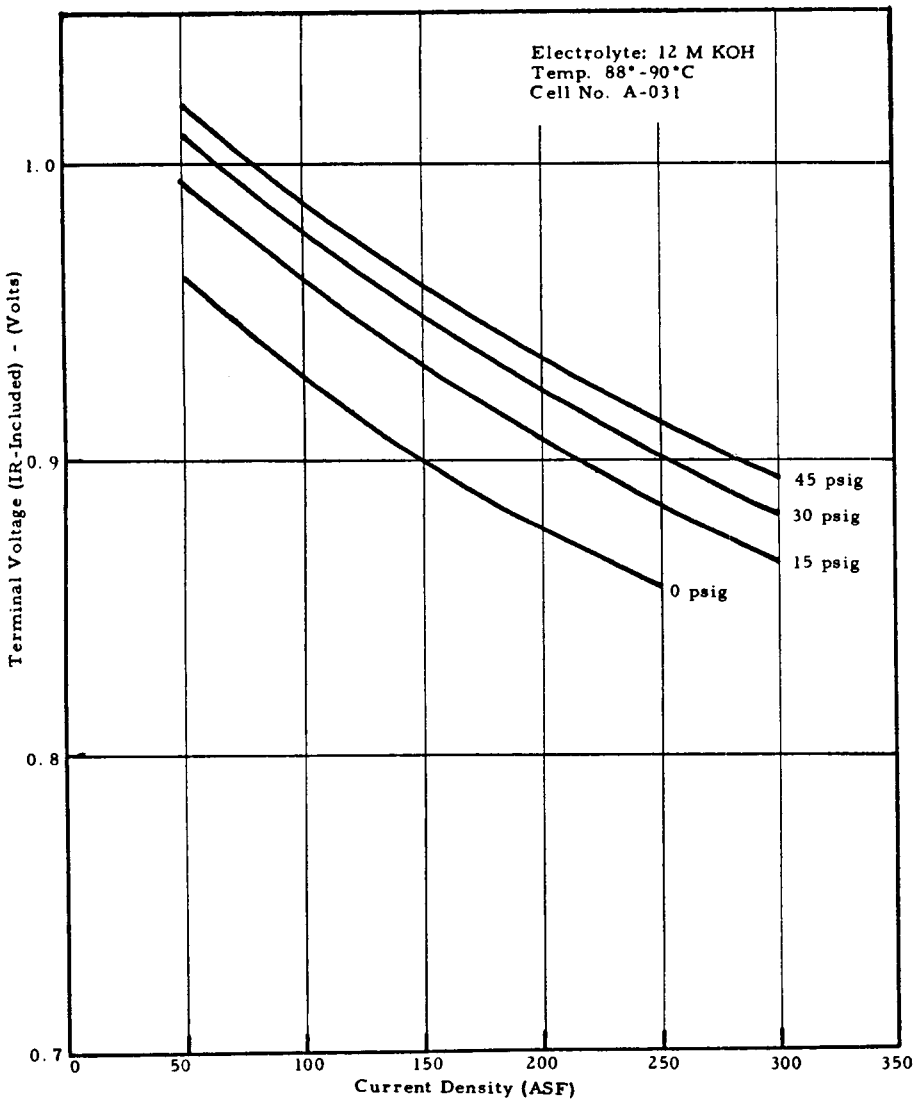

D-3096

Fig. 20 - Terminal Voltage Versus Pressure.

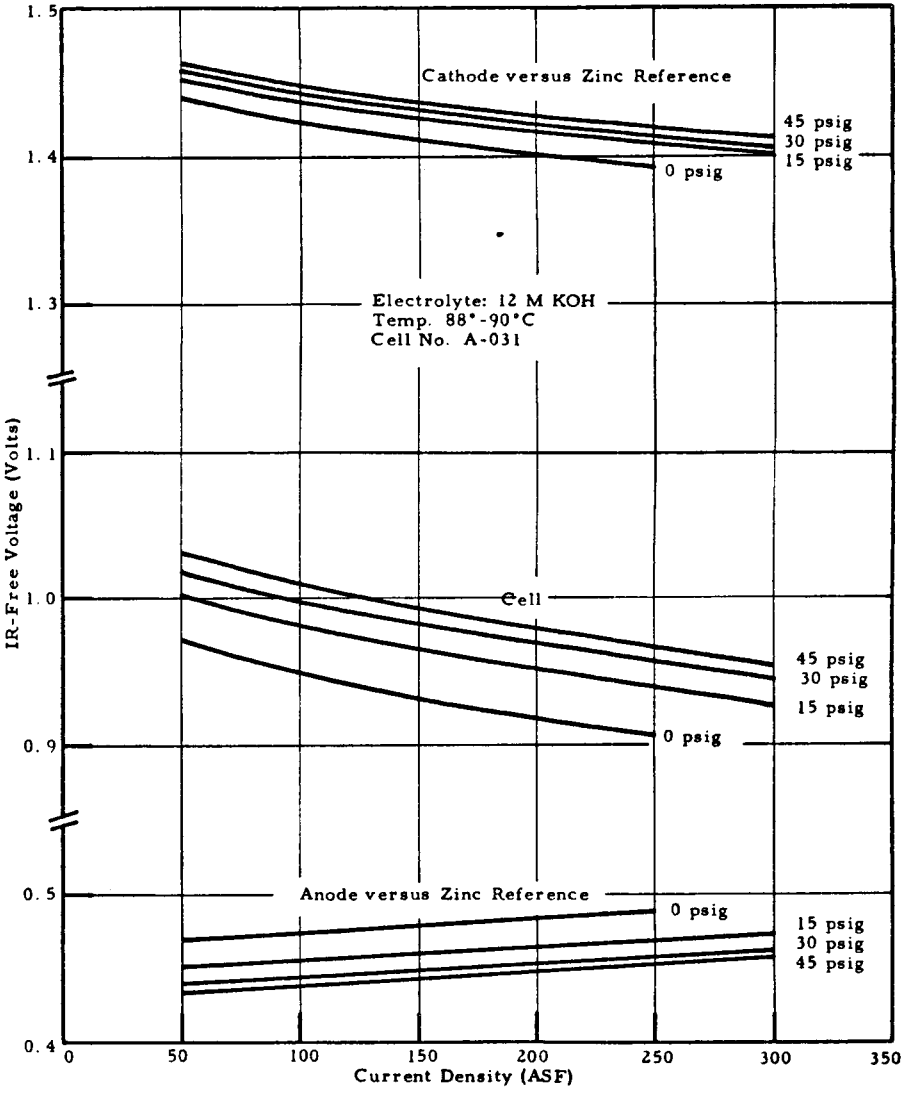

D-3095

Fig. 21 - Electrode Polarization Versus Pressure.

This possible improvement in terminal voltage would have to be traded off against several important disadvantages. An operating temperature of 130°C requires the use of highly concentrated electrolyte, leading to the danger of freeze-up during shutdown, and introduces a requirement for more complex and sensitive controls. The effect of electrolyte concentration on cell voltage increases rapidly with increasing temperature, calling for much closer tolerances on the water removal equipment and associated controls. Corrosion phenomena (or any other degradation in materials properties) become in general more severe as the temperature increases, with a resulting hazard to cell life and reliability.

In the absence of a detailed operational specification concerning start-up and shut-down capability, it has been assumed that the system should be capable of cooling without freeze-up at least to 0°C. This in turn sets a maximum KOH concentration of about 48% (about 12.4 M). The actual concentration value chosen for design purposes must be somewhat less than this, in the 11 - 12 M range, to provide some tolerance for electrolyte dilution during transients in following load changes. For a KOH concentration in this range, it can be seen from Fig. 19 that the optimum voltage is realized in the 90-100°C range. In order to minimize the possible deleterious effects of elevated temperature upon materials of construction or cell life, and also to minimize the effect of concentration upon cell voltage, the lower end of this range (90°C) has been selected as the design temperature.

6. Cell Resistance.

Significant information concerning electrode resistance has been obtained indirectly from comparison of IR-free and IR-included cell voltage data. Table VII summarizes this information. Cells employing LAB-40 electrodes have shown the lowest IR-drop readings, and have not shown much change with time. LAB-40 electrodes employ a heavy gold-plated nickel screen, and the use of pure platinum (undiluted by carbon) probably helps in lowering the electrode resistance. The stability of the cell IR-drop measurements with time demonstrates the suitability of the cell construction design (i. e., silver frames and tabs cemented to the electrodes with conductive silver epoxy).

The hybrid Type-5 cathode/Type-2 anode cells showed IR drops of about twice those of LAB-40 cells. Although testing of these cells has been of short duration, the results indicate little change in cell resistance with time, and as noted in the table, resistance decrease has actually been observed in two cases.

TABLE VII

IR-DROP MEASUREMENTS-NASA CELLS-200 ASF, 15 PSIA

Cell Description	Average Initial IR Drop	Remarks
Type-2 Cathodes Type-2 Anodes Porous Ni + Ag Frames (both electrodes)	79 mv (3 cells: 98-99°C)	Cell A-009 increased from 80 to 125 mv in 4 days; Cell A-016 increased from 75 to 177 mv in 3 days.
Type-2 Cathodes Type-2 Anodes Porous Ag (Cathodes)	67 mv (4 cells: 83-101°C)	Cell A-002 increased from 64 to 76 mv in 2 days; Cell A-003 increased from 52 to 71 mv in 1 day.
Type-5 Cathodes (on Au-plated Ag screens) Type-2 Anodes	88 mv (5 cells: 88-92°C)	After 1-2 days on test, resistance changes were small (except for one cell which had different carbon-binder ratio), and in two cases actually decreased.
LAB-40 Cells	45 mv (7 cells: 89-102°C)	Resistance increases small; only 3-6 mv in periods ranging from 2-11 days (5 cells).

Since cells made with Type-2 anodes and Type-2 cathodes have shown very large IR-drop increases with time, it seems conclusive that the resistance of the carbon-nickel bond in the Type-2 cathode increases (probably because of Ni oxidation), while the anode C-Ni bond is unaffected. This is further substantiated by the smaller effects observed when porous Ni was replaced by porous silver (see Table VII).

E. Materials Testing.

Operation at temperatures of 90°C or higher requires evaluation of the stability of cell construction materials under simulated conditions of use. A routine testing procedure has been established to check such parts as frame materials, gaskets, separators, adhesives, etc. More detailed study has been conducted to evaluate means of protecting cathode current collectors from attack by hot electrolyte in the presence of oxygen.

"Weeping" of electrodes (formation of droplets of moisture on the gas face) has been identified as an important problem area for electrodes of Type-5 and LAB-40. Since both of these electrode types employ porous Teflon as the moisture barrier, a study of available grades and types of porous Teflon has been initiated. The first step has been the measurement of such properties as porosity, per-

meability and micropore distribution, as a means of defining useful specifications for these properties in the processing or procurement of electrode materials.

1. Cell Materials.

Materials for use in cell fabrication are being tested in glass-covered Ni cylinders containing 200 ml of 12 M KOH. These cylinders are heated at 100°C for one week. Tested materials are then removed from the electrolyte, carefully washed and dried, and then investigated for any changes in physical properties. The electrolyte is examined for changes in surface tension, equlibrating molarity, and chemical contamination. From the entire group of samples tested to date only Phenoxy A, polypropylene woven-screen Lamports No. 7700, and Panelyte No. 164 were clearly unacceptable because of physical deterioration. Only Fluoroloy, ABS, Impolene-Natural, Impolene-White, and air-dried Carboline epoxy on pure polysulfone drastically reduced the surface tension of the KOH. Results of materials checked during this period are shown in Table VIII following:

TABLE VIII

MATERIALS COMPATIBILITY TESTS

Material Tested	KOH Surface Tension (dynes/cm)	M. KOH	% Weight Change	Comments
Ni Crucible	114.3	13.8		
Unannealed Pure Polysulfone	114.0	15.5	------	No obvious physical changes. KOH clear.
Annealed Pure Polysulfone	114.2	15.4	------	Ibid
Kel-F	116.1	14.9	-0.05	Ibid
G.E. PPO Hi Frequency Insulated 681-111 (Polyphenylene Oxide)	114.0	13.6	-0.02	Ibid
PPO-Buff Color-No. 53401	113.8	14.0	-0.04	Ibid
Penton	114.4	14.3	+0.003	Ibid
UCC Epoxy (15 g #2774, 5 g #2793)	114.6	14.0	+0.35	Ibid
UCC Epoxy (50 g #2774, 14.5 g #0822)	102.4	13.9	+0.49	Physical appearance was changed from translucent whitish to translucent yellowish. No detectable physical changes. KOH clear.
UCC Epoxy (25 g #2795, 7.25 g #0822)	107.3	13.8	+0.53	Ibid, except accompanied by very slight swelling.

(Continued)

TABLE VIII

(Continued)

Material Tested	KOH Surface Tension (dynes/cm)	M. KOH	% Weight Change	Comments
Carboline XA51 Mix, 15 g Adhesive, 15 g Catalyst	107.7	13.4	+1.33	Physical appearance from a shiny dark blue to dull gray. Some slight swelling. No other obvious physical changes. KOH clear.
Baked Carboline Epoxy on Pure Polysulfone	100.8	14.8	-0.05	Physical appearance from a shiny black to a dull gray with dark patches. KOH clear.
Bulk Teflon Rods	114.5	13.8	-0.05	Physical appearance became slightly more white as though slight clearing occurred. No other obvious physical changes. KOH clear.
Bulk Nylon Rods	116.0	14.5	-0.12	Material showed a slight yellowing. No other obvious changes. KOH clear.
Natural Polypropylene Tubing; Mfgr: Allied Resin; Suppliers: Aetna Plastic or Cadillac Plastics	97.6	14.2	-0.18	Physical appearance was changed from translucent white to translucent yellow. No other obvious changes. KOH clear.
Polypropylene Electrolyte Spacer	111.6	14.3	-0.23	Physical appearance from clear transparent grid to slightly yellowish, more opaque grid. No obvious strength or dimensional changes. KOH clear.
Rulon A	117.1	15.5	+0.21	KOH did not readily wash off when handled in normal manner. Crystals adhered to surface upon drying. Diam. increase of 0.77%. Color change: dark red to mottled red. KOH clear.
304 Stainless Steel	115.1	14.6	-0.02	No obvious physical change. Gray coating on surface easily wiped off. Yellow color imparted to KOH.

(Continued)

TABLE VIII

(Continued)

Material Tested	KOH Surface Tension (dynes/cm)	M. KOH	% Weight Change	Comments
Handy & Harmon No. 630; Braze on Ni-200 Sheet	116.6	14.9	------	No obvious physical change. Milky color imparted to KOH.
Ni Screen-Chore Girl	113.6	----	+0.17	Material discolored (as oxidation) and embrittled. KOH clear.
Fluoroloy	73.8	13.8	+0.03	No obvious physical change. KOH clear.
ABS	68.4	14.1	+0.03	Physical appearance from shiny reflective black to dull mat black. Slight swelling (~1.5%) in thickness. No other obvious change. KOH clear.
Impolene(Polypropylene) Tubing-Natural; Mfgr: Imperial-Eastman	74.6	13.9	-0.28	No obvious physical change. Slight yellowish stain on material. KOH clear.
Impolene (Polypropylene) Tubing-White; Mfgr: Imperial-Eastman	66.8	14.4	-0.40	No obvious physical change. Slight yellowish stain on material. KOH clear.
Air-Dried Carboline Epoxy on Pure Polysulfone	81.4	15.0	-0.17	Physical appearance from shiny black to dull gray with black patches. KOH clear.
Phenoxy A	97.3	13.9	+2.10	Physical appearance from clear transparent sheet to translucent whiteish sheet. Lost strength, became brittle, tore easily. Thickness increase ~25%. KOH clear. Unacceptable
Polypropylene Woven Screen (Lamports-7700)	104.2	13.7	-0.41	Appearance from a white opaque to yellow opaque. Lost strength, became brittle, broke with slight pressure. Less than 1/2 sample below KOH surface. KOH clear. Unacceptable.
Panelyte No. 164	104.0	14.4	+0.68	Lost smooth green lacquer coating leaving rough tan woven structure. Swelling: ~20%(edges) - ~8%(center). Edges powdery; KOH clear. Unacceptable.

Electrochemical oxidation resistance studies, directed toward employing silver current collector members in high current electrodes, have shown severe attack and disintegration of gold-plated silver samples. Expanded metal collector plates fabricated from commercial stocks of nickel and silver were gold plated at deposit levels summarized in Table IX.

TABLE IX

GOLD PLATE DEPOSIT - COLLECTOR MESH

Material	Material Designation	Piece Size	Gold Deposit - grams			
			No. 1	No. 2	No. 3	No. 4
Nickel	5 Ni 7-4/0	9" x 6"	0.20	0.41	0.82	1.60
Silver	5 Ag 7-4/0	9" x 5-1/2"	0.20	0.42	0.86	1.62

Gold-plated samples removed from the parent stock in Table IX were subjected to thermal processing to simulate conditions met in electrode preparation. A distinct color change is evident in the silver mesh after the thermal cycle, brought about by suspected alloying of the gold plate and silver substrate. Gold-plated nickel samples do not undergo an appearance change.

Electrochemical oxidation of the test samples was determined by subjecting thermally processed samples to anodic polarizing currents of 100 ASF for a two-week period in 12 M potassium hydroxide electrolyte. Temperatures were maintained at 60 to 65°C. Under these conditions oxygen is continually discharged from the test sample.

Post-test examination of the test samples revealed gross disintegration of gold-plated silver samples, irrespective of plating level. Mesh structure remaining in the sample mounts is brittle and lacks physical integrity. Evidence of electrochemical solution is apparent by deposits plated on the oxygen counter-electrode.

Nickel samples are free of any of the defects apparent in the silver samples. No advantage is noted in plating levels above the minimum examined. All samples have a nonadherent deposit on the surface which readily brushes off. No attack is visually evident with this structure.

Protection of the silver base metal by nickel plating prior to gold plating to prevent alloying is being examined.

2. Porous Teflon.

Uniformity of pore size is considered an important factor in determining the leakage characteristics of a porous structure. For this reason porous Teflon samples obtained from Chemplast and Chemical Rubber were evaluated with a number of tests designed to measure various features of the pore structure. The alcohol leak test measures both the isolated defects and the larger portion of the distribution which contributes significantly to flow. The permeability test provides specific flow data and a measure of the average pore size which is effective in determining the flow. The mercury intrusion data effectively measures the same parameters as the flow measurement, but can give added information regarding the series uniformity of the strucutre. The data in Table X below show the results of these tests.

TABLE X

PORE SIZE MEASUREMENTS

Material	Pore Diam. (μ) by Indicated Test				Air Permeability cc/cm^2/min/cm Hg
	Alcohol Max.	Alcohol Avg.	Hg Intrusion	Air Permeability	
Chemplast- Extra Fine Zitex E1002-15	16.5	12.0	15.8	----	---
Chemplast- Fine Zitex E-606A-122	18.3	11.2	18.2	8.6	155
Chemplast - Medium As Received	37.8	16.1	20.0	11.7	396
Chemplast - Medium Preshrunk	33.0	13.5	24.8	12.5	448
Chemical Rubber 150 mm - Medium	31.4	14.7	23.8	13.5	435

These data indicate that there is a somewhat finer structure associated with the fine grades of porous Teflon but the differences are not large. There seems to be no basic difference between the Chemplast and Chemical Rubber products. The major improvement of the fine grades over the medium grades of Teflon is the elimination of large defects (>1 mil diam. holes). However, defects approaching a 1-mil diameter are still evident in the fine structures.

The values of average pore diameter given by the alcohol test or the air permeability test are probably more accurate than those given by the mercury intrusion method, which tends to give high values of the average when testing thin sheets

of a soft material such as porous Teflon. This results from artifically high readings in the very-high pore size region, weighting the average to the high side. While the average is probably of dubious accuracy, the shape of the distribution curve for pore size is probably accurate in the region of small pores. Computer sheets showing the features of this distribution are included as Tables XI through XV.

The most obvious feature of each of the pore size spectra is the extremely broad distribution of pore sizes, with little evidence of the hoped-for "peaks" within the desire pore size range.

Air permeability data for the Zitex Extra Fine E1002-15 is not considered reliable; the rather thin and flimsy material showed abnormally high air flow rates suggestive of pinholes or ruptures in the sheet, possibly induced by pressure differentials intrinsic in the test method.

TABLE XI

CHEMPLAST-EXTRA FINE-ZITEX E1002-15

SAMPLE WEIGHT = .0577 GRAMS.
SAMPLE VOLUME = .0827 CC.
SURFACE AREA = 3.571 SQUARE METERS PER GRAM.
TOTAL VOLUME INTRUDED = .0558 CC.
AVERAGE PORE RADIUS = 7.902 MICRONS.

BULK DENSITY AT 100 MICRONS = .6975 G/CC.
BULK DENSITY AT 0.02 MICRONS = 2.1495 G/CC.
VOLUME OF PORES BETWEEN 100 MICRONS AND 0.020 MICRONS = .9682 CC/G.

RANGE PORE DIAMETER MICRONS	AVERAGE PORE DIAMETER MICRONS	PORE VOLUME CC/CC	CUMULATIVE PORE VOLUME CC/CC	PER CENT CUMULATIVE PORE VOLUME CC/CC	PORE VOLUME CC/CC/MICRON	PORE VOLUME CC/GRAM	CUMULATIVE PORE VOLUME CC/GRAM
100.000- 50.000	75.0000	.05113	.05113	7.57	.00102	.0733	.9682
50.000- 25.000	37.5000	.08451	.13564	20.08	.00338	.1211	.8949
25.000- 20.000	22.5000	.02245	.15810	23.40	.00449	.0321	.7738
20.000- 15.000	17.5000	.05933	.21743	32.19	.01186	.0850	.7416
15.000- 10.000	12.5000	.07274	.29018	42.96	.01454	.1042	.6565
10.000- 5.000	7.5000	.08458	.37476	55.48	.01691	.1212	.5522
5.000- 4.000	4.5000	.02605	.40082	59.34	.02605	.0373	.4310
4.000- 3.000	3.5000	.03621	.43703	64.70	.03621	.0519	.3937
3.000- 2.000	2.5000	.06730	.50434	74.66	.06730	.0964	.3417
2.000- 1.000	1.5000	.08622	.59056	87.43	.08622	.1236	.2452
1.000- .800	.9000	.01756	.60813	90.03	.08782	.0251	.1216
.800- .600	.7000	.01862	.62675	92.78	.09310	.0266	.0965
.600- .500	.5500	.00989	.63665	94.25	.09896	.0141	.0698
.500- .400	.4500	.00661	.64326	95.23	.06613	.0094	.0556
.400- .350	.3749	.00897	.65223	96.56	.17941	.0128	.0461
.350- .300	.3250	.00000	.65223	96.56	.00000	.0000	.0332
.300- .280	.2900	.00000	.65223	96.56	.00000	.0000	.0332
.280- .260	.2700	.00000	.65223	96.56	.00000	.0000	.0332
.260- .240	.2499	.00000	.65223	96.56	.00000	.0000	.0332
.240- .220	.2300	.00000	.65223	96.56	.00000	.0000	.0332
.220- .200	.2100	.00000	.65223	96.56	.00000	.0000	.0332
.200- .180	.1900	.00497	.65720	97.29	.24854	.0071	.0332
.180- .160	.1700	.00000	.65720	97.29	.00000	.0030	.0261
.160- .140	.1500	.00000	.65720	97.29	.00000	.0000	.0261
.140- .120	.1300	.00000	.65720	97.29	.00000	.0000	.0261
.120- .100	.1100	.00000	.65720	97.29	.00000	.0000	.0261
.100- .080	.0900	.00636	.66356	98.23	.31810	.0091	.0261
.080- .060	.0700	.00328	.66684	98.72	.16407	.0047	.0170
.060- .050	.0550	.00578	.67262	99.58	.57807	.0082	.0123
.050- .040	.0450	.00000	.67262	99.58	.00000	.0000	.0040
.040- .030	.0350	.00000	.67262	99.58	.00000	.0000	.0040
.030- .020	.0250	.00283	.67546	99.99	.28339	.0040	.0040

TABLE XII

CHEMPLAST-FINE-ZITEX E-606A-122

SAMPLE WEIGHT = .1267 GRAMS.
SAMPLE VOLUME = .1515 CC.
SURFACE AREA = 2.079 SQUARE METERS PER GRAM.
TOTAL VOLUME INTRUDED = .0933 CC.
AVERAGE PORE RADIUS = 9.111 MICRONS.

BULK DENSITY AT 100 MICRONS = .8364 G/CC.
BULK DENSITY AT 0.02 MICRONS = 2.1779 G/CC.
VOLUME OF PORES BETWEEN 100 MICRONS AND 0.020 MICRONS = .7363 CC/G.

RANGE PORE DIAMETER MICRONS	AVERAGE PORE DIAMETER MICRONS	PORE VOLUME CC/CC	CUMULATIVE PORE VOLUME CC/CC	PER CENT CUMULATIVE PORE VOLUME CC/CC	PORE VOLUME CC/CC/MICRON	PORE VOLUME CC/GRAM	CUMULATIVE PORE VOLUME CC/GRAM
100.000- 50.000	75.0000	.06212	.06212	10.08	.00124	.0742	.7363
50.000- 25.000	37.5000	.08516	.14729	23.91	.00340	.1018	.6621
25.000- 20.000	22.5000	.04437	.19166	31.11	.00887	.0530	.5602
20.000- 15.000	17.5000	.04391	.23557	38.24	.00878	.0524	.5072
15.000- 10.000	12.5000	.03443	.27001	43.83	.00688	.0411	.4547
10.000- 5.000	7.5000	.06398	.33399	54.22	.01279	.0764	.4135
5.000- 4.000	4.5000	.03673	.37073	60.18	.03673	.0439	.3370
4.000- 3.000	3.5000	.07053	.44126	71.63	.07053	.0843	.2931
3.000- 2.000	2.5000	.07065	.51191	83.10	.07065	.0844	.2088
2.000- 1.000	1.5000	.05425	.56616	91.91	.05425	.0648	.1243
1.000- .800	.9000	.00963	.57579	93.48	.04815	.0115	.0595
.800- .600	.7000	.01017	.58597	95.13	.05088	.0121	.0480
.600- .500	.5500	.00543	.59140	96.01	.05436	.0064	.0358
.500- .400	.4500	.00360	.59501	96.60	.03609	.0043	.0293
.400- .350	.3749	.00492	.59994	97.40	.09856	.0058	.0250
.350- .300	.3250	.00000	.59994	97.40	.00000	.0000	.0191
.300- .280	.2900	.00000	.59994	97.40	.00000	.0000	.0191
.280- .260	.2700	.00087	.60082	97.54	.04395	.0010	.0191
.260- .240	.2499	.00258	.60340	97.96	.12909	.0030	.0180
.240- .220	.2300	.00296	.60637	98.44	.14817	.0035	.0149
.220- .200	.2100	.00000	.60637	98.44	.00000	.0000	.0114
.200- .180	.1900	.00000	.60637	98.44	.00000	.0000	.0114
.180- .160	.1700	.00000	.60637	98.44	.00000	.0000	.0114
.160- .140	.1500	.00000	.60637	98.44	.00000	.0000	.0114
.140- .120	.1300	.00000	.60637	98.44	.00000	.0000	.0114
.120- .100	.1100	.00000	.60637	98.44	.00000	.0000	.0114
.100- .080	.0900	.00062	.60700	98.54	.03145	.0007	.0114
.080- .060	.0700	.00289	.60989	99.01	.14477	.0034	.0107
.060- .050	.0550	.00152	.61141	99.26	.15230	.0016	.0072
.050- .040	.0450	.00059	.61201	99.36	.05927	.0007	.0054
.040- .030	.0350	.00259	.61460	99.78	.25972	.0031	.0047
.030- .020	.0250	.00134	.61595	99.99	.13415	.0016	.0016

TABLE XIII

CHEMPLAST-MEDIUM-AS RECEIVED

SAMPLE WEIGHT = .0835 GRAMS.
SAMPLE VOLUME = .1224 CC.
SURFACE AREA = 2.965 SQUARE METERS PER GRAM.
TOTAL VOLUME INTRUDED = .0818 CC.
AVERAGE PORE RADIUS = 10.066 MICRONS.

BULK DENSITY AT 100 MICRONS = .6821 G/CC.
BULK DENSITY AT 0.02 MICRONS = 2.0574 G/CC.
VOLUME OF PORES BETWEEN 100 MICRONS AND 0.020 MICRONS = .9798 CC/G.

RANGE PORE DIAMETER MICRONS	AVERAGE PORE DIAMETER MICRONS	PORE VOLUME CC/CC	CUMULATIVE PORE VOLUME CC/CC	PER CENT CUMULATIVE PORE VOLUME CC/CC	PORE VOLUME CC/CC/MICRON	PORE VOLUME CC/GRAM	CUMULATIVE PORE VOLUME CC/GRAM
100.000- 50.000	75.0000	.07991	.07991	11.95	.00159	.1171	.9798
50.000- 25.000	37.5000	.07615	.15607	23.34	.00304	.1116	.8626
25.000- 20.000	22.5000	.04509	.20117	30.09	.00901	.0661	.7510
20.000- 15.000	17.5000	.08517	.28634	42.83	.01703	.1248	.6849
15.000- 10.000	12.5000	.07292	.35927	53.74	.01458	.1069	.5600
10.000- 5.000	7.5000	.09253	.45180	67.59	.01850	.1356	.4531
5.000- 4.000	4.5000	.03043	.48224	72.14	.03043	.0446	.3175
4.000- 3.000	3.5000	.04156	.52380	78.36	.04156	.0609	.2729
3.000- 2.000	2.5000	.04791	.57172	85.53	.04791	.0702	.2119
2.000- 1.000	1.5000	.04781	.61954	92.68	.04781	.0700	.1417
1.000- .800	.9000	.01181	.63135	94.45	.05906	.0173	.0716
.800- .600	.7000	.00567	.63703	95.30	.02839	.0083	.0543
.600- .500	.5500	.00285	.63988	95.73	.02852	.0041	.0460
.500- .400	.4500	.00981	.64969	97.19	.09813	.0143	.0418
.400- .350	.3749	.00350	.65319	97.72	.07002	.0051	.0274
.350- .300	.3250	.00000	.65319	97.72	.00000	.0000	.0223
.300- .280	.2900	.00000	.65319	97.72	.00000	.0000	.0223
.280- .260	.2700	.00000	.65319	97.72	.00000	.0000	.0223
.260- .240	.2499	.00000	.65319	97.72	.00000	.0000	.0223
.240- .220	.2300	.00000	.65319	97.72	.00000	.0000	.0223
.220- .200	.2100	.00000	.65319	97.72	.00000	.0000	.0223
.200- .180	.1900	.00000	.65319	97.72	.00000	.0000	.0223
.180- .160	.1700	.00000	.65319	97.72	.00000	.0000	.0223
.160- .140	.1500	.00000	.65319	97.72	.00000	.0000	.0223
.140- .120	.1300	.00000	.65319	97.72	.00000	.0000	.0223
.120- .100	.1100	.00000	.65319	97.72	.00000	.0000	.0223
.100- .080	.0900	.00752	.66072	98.84	.37614	.0110	.0223
.080- .060	.0700	.00000	.66072	98.84	.00000	.0000	.0112
.060- .050	.0550	.00000	.66072	98.84	.00000	.0000	.0112
.050- .040	.0450	.00213	.66285	99.16	.21301	.0031	.0112
.040- .030	.0350	.00276	.66561	99.57	.27626	.0040	.0081
.030- .020	.0250	.00281	.66842	99.99	.28106	.0041	.0041

TABLE XIV

CHEMPLAST-MEDIUM-PRESHRUNK

SAMPLE WEIGHT = .0718 GRAMS.
SAMPLE VOLUME = .1088 CC.
SURFACE AREA = 1.049 SQUARE METERS PER GRAM.
TOTAL VOLUME INTRUDED = .0739 CC.
AVERAGE PORE RADIUS = 12.431 MICRONS.

BULK DENSITY AT 100 MICRONS = .6598 G/CC.
BULK DENSITY AT 0.02 MICRONS = 2.0590 G/CC.
VOLUME OF PORES BETWEEN 100 MICRONS AND 0.020 MICRONS = 1.0299 CC/G.

RANGE PORE DIAMETER MICRONS	AVERAGE PORE DIAMETER MICRONS	PORE VOLUME CC/CC	CUMULATIVE PORE VOLUME CC/CC	PER CENT CUMULATIVE PORE VOLUME CC/CC	PORE VOLUME CC/CC/MICRON	PORE VOLUME CC/GRAM	CUMULATIVE PORE VOLUME CC/GRAM
100.000- 50.000	75.0000	.11626	.11626	17.10	.00232	.1762	1.0299
50.000- 25.000	37.5000	.10836	.22463	33.05	.00433	.1642	.8536
25.000- 20.000	22.5000	.04824	.27288	40.15	.00964	.0731	.6894
20.000- 15.000	17.5000	.05675	.32963	48.50	.01135	.0860	.6163
15.000- 10.000	12.5000	.06233	.39197	57.68	.01246	.0944	.5303
10.000- 5.000	7.5000	.09859	.49057	72.19	.01971	.1494	.4358
5.000- 4.000	4.5000	.04303	.53360	78.52	.04303	.0652	.2864
4.000- 3.000	3.5000	.04337	.57698	84.90	.04337	.0657	.2211
3.000- 2.000	2.5000	.03888	.61586	90.62	.03888	.0589	.1554
2.000- 1.000	1.5000	.03995	.65582	96.50	.03995	.0605	.0965
1.000- .800	.9000	.00564	.66146	97.33	.02821	.0085	.0359
.800- .600	.7000	.00000	.66146	97.33	.00000	.0000	.0274
.600- .500	.5500	.00320	.66466	97.81	.03205	.0048	.0274
.500- .400	.4500	.00579	.67046	98.66	.05792	.0087	.0225
.400- .350	.3749	.00000	.67046	98.66	.00000	.0000	.0137
.350- .300	.3250	.00000	.67046	98.66	.00000	.0000	.0137
.300- .280	.2900	.00000	.67046	98.66	.00000	.0000	.0137
.280- .260	.2700	.00124	.67170	98.84	.06211	.0018	.0137
.260- .240	.2499	.00355	.67526	99.36	.17794	.0053	.0118
.240- .220	.2300	.00405	.67931	99.96	.20264	.0061	.0064
.220- .200	.2100	.00000	.67931	99.96	.00000	.0000	.0003
.200- .180	.1900	.00000	.67931	99.96	.00000	.0000	.0003
.180- .160	.1700	.00000	.67931	99.96	.00000	.0000	.0003
.160- .140	.1500	.00000	.67931	99.96	.00000	.0000	.0003
.140- .120	.1300	.00000	.67931	99.96	.00000	.0000	.0003
.120- .100	.1100	.00000	.67931	99.96	.00000	.0000	.0003
.100- .080	.0900	.00000	.67931	99.96	.00000	.0000	.0003
.080- .060	.0700	.00000	.67931	99.96	.00000	.0000	.0003
.060- .050	.0550	.00000	.67931	99.96	.00000	.0000	.0003
.050- .040	.0450	.00000	.67931	99.96	.00000	.0000	.0003
.040- .030	.0350	.00000	.67931	99.96	.00000	.0000	.0003
.030- .020	.0250	.00023	.67954	99.99	.02325	.0003	.0003

TABLE XV

CHEMICAL RUBBER-150 MM-MEDIUM

SAMPLE WEIGHT = .1774 GRAMS.
SAMPLE VOLUME = .2593 CC.
SURFACE AREA = 2.155 SQUARE METERS PER GRAM.
TOTAL VOLUME INTRUDED = .1787 CC.
AVERAGE PORE RADIUS = 11.941 MICRONS.

BULK DENSITY AT 100 MICRONS = .6843 G/CC.
BULK DENSITY AT 0.02 MICRONS = 2.2030 G/CC.
VOLUME OF PORES BETWEEN 100 MICRONS AND 0.020 MICRONS = 1.0072 CC/G.

RANGE PORE DIAMETER MICRONS	AVERAGE PORE DIAMETER MICRONS	PORE VOLUME CC/CC	CUMULATIVE PORE VOLUME CC/CC	PER CENT CUMULATIVE PORE VOLUME CC/CC	PORE VOLUME CC/CC/MICRON	PORE VOLUME CC/GRAM	CUMULATIVE PORE VOLUME CC/GRAM
100.000- 50.000	75.0000	.09651	.09651	14.00	.00193	.1410	1.0072
50.000- 25.000	37.5000	.12431	.22083	32.03	.00497	.1816	.8662
25.000- 20.000	22.5000	.07773	.29857	43.31	.01554	.1135	.6845
20.000- 15.000	17.5000	.05864	.35721	51.81	.01172	.0856	.5709
15.000- 10.000	12.5000	.05881	.41602	60.35	.01176	.0859	.4852
10.000- 5.000	7.5000	.07847	.49450	71.73	.01569	.1146	.3993
5.000- 4.000	4.5000	.03267	.52718	76.47	.03267	.0477	.2846
4.000- 3.000	3.5000	.03433	.56151	81.45	.03433	.0501	.2369
3.000- 2.000	2.5000	.04428	.60579	87.88	.04428	.0647	.1867
2.000- 1.000	1.5000	.04525	.65105	94.44	.04525	.0661	.1220
1.000- .800	.9000	.00649	.65755	95.38	.03249	.0094	.0559
.800- .600	.7000	.00872	.66628	96.65	.04363	.0127	.0464
.600- .500	.5500	.00322	.66950	97.12	.03223	.0047	.0337
.500- .400	.4500	.00211	.67161	97.42	.02111	.0030	.0289
.400- .350	.3749	.00177	.67339	97.68	.03557	.0025	.0259
.350- .300	.3250	.00195	.67534	97.96	.03902	.0028	.0233
.300- .280	.2900	.00093	.67627	98.10	.04659	.0013	.0204
.280- .260	.2700	.00205	.67833	98.40	.10277	.0030	.0190
.260- .240	.2499	.00000	.67833	98.40	.00000	.0000	.0160
.240- .220	.2300	.00000	.67833	98.40	.00000	.0000	.0160
.220- .200	.2100	.00000	.67833	98.40	.00000	.0000	.0160
.200- .180	.1900	.00161	.67994	98.63	.08071	.0023	.0160
.180- .160	.1700	.00000	.67994	98.63	.00000	.0000	.0137
.160- .140	.1500	.00000	.67994	98.63	.00000	.0000	.0137
.140- .120	.1300	.00000	.67994	98.63	.00000	.0000	.0137
.120- .100	.1100	.00000	.67994	98.63	.00000	.0000	.0137
.100- .080	.0900	.00554	.68549	99.44	.27737	.0081	.0137
.080- .060	.0700	.00000	.68549	99.44	.00000	.0000	.0056
.060- .050	.0550	.00000	.68549	99.44	.00000	.0000	.0056
.050- .040	.0450	.00028	.68578	99.48	.02899	.0004	.0056
.040- .030	.0350	.00127	.68706	99.66	.12769	.0018	.0052
.030- .020	.0250	.00228	.68934	99.99	.22831	.0033	.0033

Task 2 - Preliminary System Design.

The second task of the present program is the preliminary design of a nominal 5-KW fuel cell power system. The system shall be designed to deliver 5000 watts continuously and have a short-term operating capability over the range from 2500 to 8000 watts at 29 ±2 volts, at a temperature approaching 100°C. The power and voltage levels specified shall be terminal quantities deliverable to an external load. The design operating point (voltage and current density) for the fuel cell shall be chosen with an objective of achieving a minimum lifetime of 3000 hours while performing the load profile shown in Fig. 22.

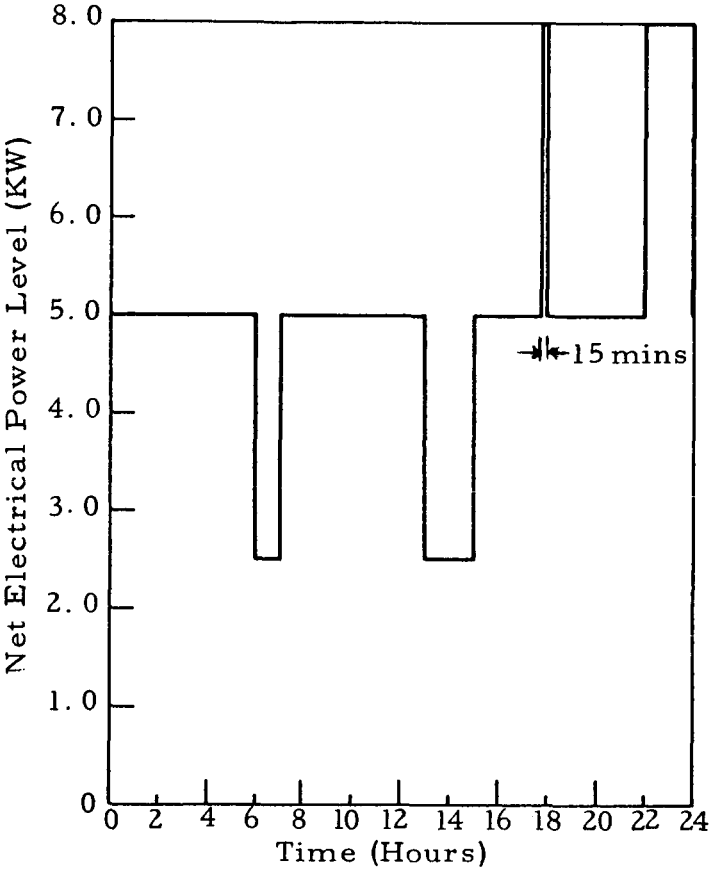

D-3143

Fig. 22 - NASA 5-KW System 24-Hour Load Duty Cycle (Cycle Repeats Every 24 Hours).

As a matter of advisory guidance to the design team, NASA has supplied a set of environmental specifications which are included as Appendix A of this report.

In accordance with the approved schedule, effort under Task 2 has been concentrated in the final six months of the program so as to make available as much cell test data as possible to guide the design effort. Some of the preliminary design data and criteria have been selected, as shown in Table XVI for the fuel cell stack, and in Table XVII for the system.

TABLE XVI

STACK DESIGN

Variables	Specifications
Nominal Design Point:	
Power Level	5 KW
Cell Terminal Voltage, Initial At 3000 hr.	0.945 v 0.875 v
Current Density, at 3000 hr	120 ASF
Power Density, Initial	113.4 w/ft^2
Operating Temperature	90°C
Maximum Overload Point	8 KW
Minimum Lifetime	3000 hours
Maximum Operating Temperature	100°C
Maximum Operating Pressure	30 psia
Stack Geometry	
Electrical Hookup	4 plates in parallel/cell 18 cells in series/stack
Electrode Area*	0.331 ft^2/electrode
Number of Stacks	2
Stack Electrical Hookup	Series

* Based on 3000-hour cell voltage at nominal design point.

TABLE XVII

SYSTEM PARAMETERS

Variables	Specifications
Design Center Power	5 KW, continuous
Power Range, Short-term	2.5 - 8.0 KW
Voltage	29 ± 2 volts
Lifetime	3000 hours
Coolant	Water
Coolant Flow Available	500 lb/hr
Inlet Coolant Temperature	75°F, maximum
Condensate Reservoir Capacity	56 lb
Fuel	H_2 supplied at 140 psia, minimum; at 40°F minimum
Oxidant	O_2 supplied at 140 psia, minimum; at 40°F minimum

Based on a 30 psia operating pressure and 90°C operating temperature, the polarization curve shown in Fig. 23 has been selected for use in preliminary design. Degradation of voltage with time has been based on an assumed 4 mv/100 hours loss at the 200 ASF point. The "initial" polarization curve in this figure corresponds closely with that of Cell A-015 initially; since this cell test was conducted at 15 psia and the preliminary design is based on 30 psia operation, there is a slight (about 10 mv at 200 ASF) safety factor built into the design curve. Cell A-015 at 800 hours is operating at 12 mv higher than the design curve prediction (despite atmospheric pressure operation). Considering the inevitable minor losses in voltage in going from a "best" test cell to a full-scale stack the design curves are considered to be a realistic projection.

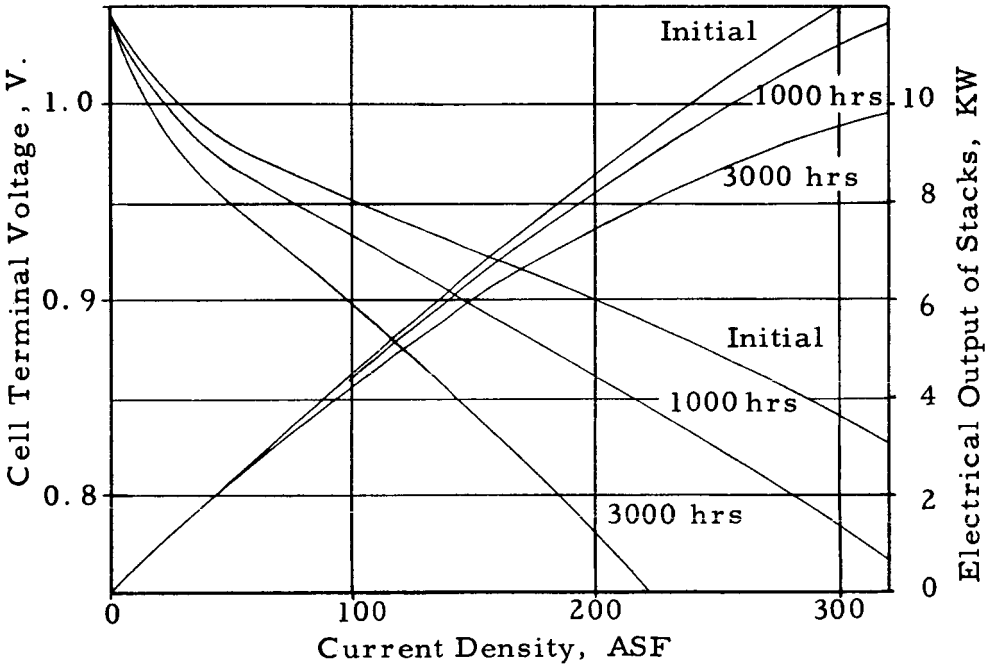

D-3142

Fig. 23 - NASA 5-KW System Polarization Curves.

Accumulation of additional cell test data will, of course, permit a more definitive projection of the system performance characteristics than is possible at the present time.

Plans have been made to subcontract design of the "Thermal Control Subsystem" to the AiResearch Manufacturing Division of the Garrett Corporation. This subsystem provides removal of water from one or both reactant streams, storage of collected condensate, and control of temperature and removal of entrained gas from the circulating KOH stream. A set of interface specifications have been developed to guide this portion of the effort and are included in Appendix B.

PLANS FOR FUTURE WORK

Effort under the Task 1-Electrode Improvement program will continue with further testing of small (4" x 4-1/2") cells. This effort has two objectives; first, to verify improvements in electrode quality, uniformity, and performance resulting from changes in specifications or fabrication techniques, and second, to collect performance data over a broad range of operating conditions to guide the system engineering design effort. Improvements in electrode quality will be measured against a routine 200 ASF life test. Cell tests under controlled variations in temperature, electrolyte concentration, fluid flow rates, etc., will provide a preliminary definition of optimum design center values and tolerances on these variables. Testing of cell materials will be continued to collect the data required for the establishment of a bill-of-qualified-materials covering all of the essential materials of the fuel cell. An important by-product of this test program is the validation and refining of test procedures, leading to an accumulation of data which will provide a rational basis for establishing future inspection and acceptance test procedures, and which will permit the writing of realistic materials specifications.

Effort under the Task 1 program will culminate in the performance testing of "flight-size" cells (i. e., one square foot of anode and cathode area per cell). Design of these cells will be based on data collected from 4" x 4-1/2" cell tests plus engineering calculations to establish reasonable values for geometric parameters, current collector configuration, fluid entrance and exit ports, etc.

Work has just been initiated on the Task 2-Preliminary System Design. This effort will include:

1. Development of an overall system schematic and flow diagram describing water removal and temperature control subsystems and including all fluid and coolant flow rates, and giving fluid types, temperatures, and pressures representative of operation to the load profile shown in Fig. 22.
2. Preparation of an assembly drawing of the electrochemical cells, including reactant manifolding, electrolyte manifolding, and recommended series-parallel electrical connections, to obtain a 29-volt DC stack capable of delivering 5,000 watts.

3. Development of a control schematic, including identification of control and sensing elements, variables to be controlled, mode of control, and acceptable operating range for each system component.

4. Identification of all system components whose operation is dependent upon, or influenced by gravity.

5. Preparation of a source list for all items to be used in assembly of the system hardware. This list shall include:

   a. Identification of components the Contractor proposes to supply.

   b. Identification of those components which the Contractor anticipates may be purchased in a form suitable to fully meet the requirements of the environmental specification.

APPENDIX A

ENVIRONMENTAL SPECIFICATIONS

All environmental tests described below are assumed to be conducted at a test temperature of 20°C. All tests shall be non-operating tests. Components which contain fluid in normal service shall be filled with the proper fluid to simulate service conditions.

1. Shock

   The test piece shall be securely mounted in a test fixture specifically designed to support the piece in each of three perpendicular axes for shock testing. The test piece shall remain inoperative throughout the shock tests.

   Three shock impulses of 18 g's shall be applied to the test piece along each of the three perpendicular axes in each direction making a total of 18 shock impulses per cell. Each input pulse waveshape will be a half-sine pulse for a time duration of eight milliseconds.

2. Vibration

   The test piece shall be securely mounted in a text fixutre specifically designed to support the piece in any of the three mutually perpendicular axes for vibration tests. The test piece shall remain inoperative throughout the vibration tests.

   A resonant survey test will be performed to determine the resonant modes of the test fixture and piece. A frequency sweep will be made from 10 to 24.5 cps with a displacement amplitude of 0.50 inch peak to peak from 24.5 to 3000 cps at 15 g, zero to peak. This frequency sweep shall be performed once along each of the three mutually perpendicular axes. During each frequency sweep all resonant frequency points shall be recorded. The duration of each frequency sweep in each axis shall be one minute from 10 to 24.5 cps and ten minutes from 24.5 to 3000 cps. A resonant frequency test at one-half of each resonant frequency resulting from the resonant frequency sweep noted above, shall be performed for a period of 30 minutes for each resonant frequency.

3. Acoustic Noise

   The test piece shall be securely mounted in a test fixture specifically designed to support the piece in any of the three mutually perpendicular axes for the

acoustic noise tests. An acoustic noise chamber shall be used for these tests. The test piece shall remain inoperative throughout the acoustic noise tests.

An acoustic noise test shall be performed by applying a total integrated sound pressure level of 148 decibels, Re 0.0002 micro bar with a frequency spectrum as shown in Fig. 24 for a period not less than five minutes. The test shall be performed in each of the three mutually perpendicular axes.

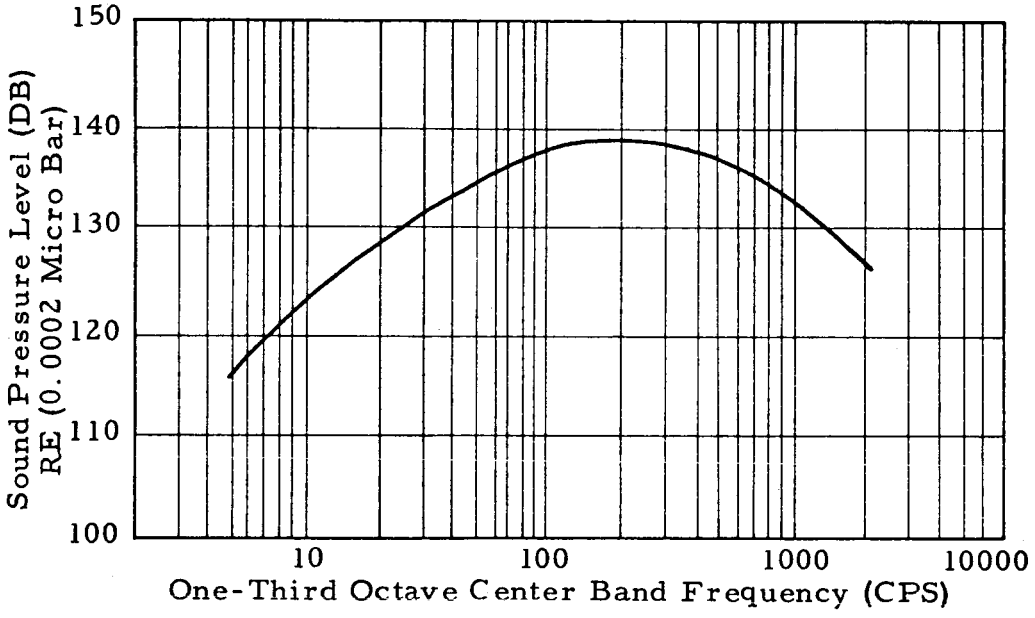

D-3184

Fig. 24 - Acoustic Noise Frequency Spectrum.

4. Acceleration

The test piece shall be securely mounted in a test fixture specifically designed to support the piece in any of the three mutually perpendicular axes for the acceleration tests. The test piece shall remain electrically inoperative throughout the acceleration tests.

Acceleration tests shall be performed in accordance with the following procedure:

a. A sustained acceleration force of 18 g's shall be applied for five minutes along the longitudinal axis chosen in a direction simulating the lift-off of the transporting space vehicle.

b. A sustained acceleration force of 18 g's shall be applied for five minutes along the longitudinal axis in the opposite direction to that in Item a. above.

c. A sustained acceleration force of 18 g's shall be applied for five minutes in both directions along each of the remaining two mutually perpendicular axes to the longitudinal axis of Items a. and b. above.

5. Tolerances

The following tolerances shall apply to all environmental tests unless otherwise specified:

a. Temperature, ±5°F or 3%, whichever is greater

b. Vibration Amplitude (g or inches), ±10%

c. Vibration Frequency (cps), ±2% or 1 cps, whichever is greater

d. Shock, (g) ±10%

e. Acceleration (g), ±5% at reference point

f. Sound Pressure Level, Overall (db), ±2 db

g. Sound Pressure Level, Any One Octave (db), ±3 db

APPENDIX B

SPECIFICATION NO. DD-3A
THERMAL CONTROL SUBSYSTEM FOR NOMINAL 5000-WATT AEROSPACE HYDROGEN-OXYGEN FUEL CELL POWER SUPPLY

1. Scope

This specification covers the requirements for a thermal control subsystem to be utilized with a nominal 5000-watt hydrogen-oxygen fuel cell power supply. The power supply and its associated thermal control sybsystem must be capable of operation in a space environment, including zero g.

2. Requirements

The primary functions of the thermal control sybsystem are (1) to remove water vapor from a recirculating oxygen stream; (2) to remove water vapor from a recirculating hydrogen stream; (3) to store the collected condensate, and (4) to control the temperature and remove entrained gases from a circulating potassium hydroxide stream. While fulfilling these functions the subsystem must meet the requirements set forth in this specification.

2.1 Environmental Specifications

2.1.1 Zero Gravity: The thermal control subsystem shall be operational in a zero gravity environment, and each of the components shall be operational in a 1 g environment oriented in the "neutral" attitude, i.e., perpendicular to that direction in which performance is assisted by gravity.

2.1.2 Life: The thermal control subsystem shall have an operational lifetime of 3000 hours.

2.1.3 Shock: The thermal control subsystem shall not be damaged when subjected to three shock impulses of 18 g's along each of the three perpendicular axes in each direction, i.e., a total of 18 shock impulses. Each input pulse wave shape shall be a half-sine pulse for a duration of 8 milliseconds.

2.1.4 Vibration: The thermal control subsystem shall not be damaged by a vibrational frequency sweep from 10 to 24.5 cps with a displacement amplitude of 0.50 inch peak-to-peak from 24.5 to 3000 cps at 15 g, zero to peak. The duration of each frequency

sweep in each axis shall be one minute from 10 to 24.5 cps and 10 minutes from 24.5 to 3000 cps. System must be capable of withstanding frequency sweeps along any or all of three mutually perpendicular axes. In addition, the thermal control sybsystem shall not be damaged by a resonant frequency test at one-half of each predetermined resonant frequency for a period of 30 minutes.

2.1.5 Acoustic Noise: The thermal control subsystem shall not be damaged when subjected to a total integrated sound pressure level of 148 decibels, Re 0.0002 microbar with a frequency spectrum as shown in Fig. 24 for a period not less than five minutes. This sound pressure can be applied along each of the three mutually perpendicular axes.

2.1.6 Operating Temperature: The thermal control subsystem shall be operational in ambient temperatures from +35 to 160°F.

2.1.7 Acceleration: The thermal control subsystem shall not be damaged when subjected to the following acceleration test:

(a) A sustained acceleration force of 18 g's applied for five minutes along the longitudinal axis chosen in a direction simulating the lift-off of the transporting space vehicle.

(b) A sustained acceleration force of 18 g's applied for five minutes along the longitudinal axis in the opposite direction to that in item (a) above.

(c) A sustained acceleration force of 18 g's applied for five minutes in both directions along each of the remaining two mutually perpendicular axes to the longitudinal axes of items (a) and (b) above.

2.2 Equipment

The thermal control subsystem shall include the following components:

(a) A potassium hydroxide-to-water primary heat exchanger.

(b) A means of controlling the water flow rate through the potassium hydroxide heat exchanger.

(c) A condenser for removing water vapor from a recirculating hydrogen stream.

(d) A condenser for removing water vapor from a recirculating oxygen stream.

(e) Tankage for collecting condensate.

(f) A gas-liquid separator for the circulating potassium hydroxide system.

(g) Any controls, pressure regulators or auxiliary equipment necessary for operation of items (a)-(f).

Although the thermal control subsystem has been defined as an integral unit, in order to permit maximum integration of the complete power supply, the subcontractor shall not be responsible for the design and layout of the interconnecting piping between any of the components. However, as set forth in the contract statement of work the subcontractor must supply a fluid schematic showing how the individual components must be coupled together to meet the operational and environmental requirements.

2.3 Operational and Interface Data

The thermal control sybsystem will be supplied with a maximum of 500 lb/hr of water for use as a coolant. The inlet temperature of the water stream will be 75°F maximum at a total pressure of 20 psia. The sum of the coolant pressure losses through all of the components in the thermal control subsystem (exclusive of the interconnecting piping) shall be 4.5 psi.

The subcontractor is responsible for determining the optimum interconnection scheme for the coolant system, i.e., heat exchanger coolant flow in series or in parallel, etc.

2.3.1 KOH Heat Exchanger: This exchanger shall be designed to meet the following requirements:

Maximum Heat Load	22,500 Btu/hr minus (sensible heat removed from the gas streams by the condensers whose performance is specified in paragraphs 2.3.2 and 2.3.3
KOH Flow Rate	3310 lb/hr (based on 11 N)
KOH Normality	9-12 Normal
KOH Inlet Pressure (total)	30 psia
KOH Inlet Temperature	194°F ±5°F
KOH Outlet Temperature	184° ±5°F
Maximum Permissible Pressure Drop (KOH Side)	0.85 psia

(The fuel cell power supply will operate over a varying load profile. Consequently, the required heat rejection rate for the KOH heat exchanger will vary. The data shown in para. 2.3.1 are representative of the peak duty. Although it is not expected to influence the design, the duty cycle for the heat exchanger over all operating conditions will be issued as a supplement to this specification within 15 days after the subcontractor initiates work.)

2.3.1.1 Electrical Potential: The KOH heat exchanger shall be designed so as not to be influenced by an electrical current of 2 amps which the circulating potassium hydroxide stream will be carrying.

A metal KOH heat exchanger will carry a D.C. potential because of this contact with the fuel cell electrolyte. The value of this D.C. voltage is a function of the system design and may be at any value between 0-36 volts, depending on choices of heat exchanger placement, fuel cell electrolyte feed and discharge design, etc.

2.3.2 Hydrogen Sybsystem Condenser: The hydrogen sybsystem condenser shall be designed to meet the following requirements:

Hydrogen Inlet Temperature	194°F
Hydrogen Flow Rate (as Dry Gas)	4.04 lb/hr
Inlet H_2O Partial Pressure	160 mm Hg
Hydrogen Stream Inlet Pressure (Total)	28.5 psia
H_2O Condensation Rate	3.27 lb/hr
Hydrogen Side ΔP	0.5" water max.

(As noted for the KOH heat exchanger, the hydrogen condenser duty cycle will vary as the load profile on the fuel cell is varied. The data shown in para. 2.3.2 are representative of the average condensation point. Within 15 days after the subcontractor initiates work, a supplement to this specification will be issued showing conditions for all operating points.)

2.3.3 Oxygen Subsystem Condenser: The oxygen subsystem condenser shall be designed to meet the following requirements:

Oxygen Inlet Temperature	194°F
Oxygen Flow Rate (as Dry Gas)	32.07 lb/hr
Inlet H_2O Partial Pressure	120 mm Hg
Oxygen Stream Inlet Pressure (Total)	28.5 psia
H_2O Condensation Rate	1.09 lb/hr
Oxygen Side ΔP	0.5" water max.

(As with the hydrogen subsystem condenser, the data shown in para. 2.3.2 are representative of the maximum condensation point. Within 15 days after subcontractor initiates work a supplement to this specification will be issued showing conditions for all operating points.)

2.3.4 Condensate Tankage: This tankage shall be sized to provide storage of 56 lb of water. A means shall be provided for manually dumping excess water when the 56-lb point is exceeded. A gauging system shall be included which will provide the operator with a signal so that he knows when to dump.

2.3.5 Gas-Liquid Separator: The primary function of the gas-liquid separator is to remove entrained oxygen or hydrogen from the circulating potassium hydroxide stream. A means shall be incorporated to automatically vent the collected gas to the ambient whether it be at space vacuum or 14 psia. The gas may be hydrogen or oxygen or mixtures of the two. The design of the gas-liquid separator shall consider the explosive nature of such mixtures and provisions incorporated to minimize the resultant hazards. The gas-liquid separator shall be designed to meet the following requirements:

KOH (as Liquid) Flow Rate*	3310 lb/hr
KOH Normality	9-12 Normal
KOH Temperature (Maximum)	199°F
Max. Permissible Pressure Drop	0.65 psi
Estimated Entrained Gas Content (Max. Entering Separator)	60 cc/min

* The design shall consider the fact that this KOH can contain carbon particles ranging in size up to 30 microns.

Estimated Size Range of Gas Bubbles (Entering Separator)	0.027" - 0.200" diam.
Allowable Entrained Gas Content (Leaving Separator)	0.50 cc/min.

During venting of the collected gases, loss of small quantities of KOH can be tolerated. Such losses shall not exceed 625 ml for every 1500 hours of operation.

2.3.6 Controls, Pressure Regulators and/or Auxiliary Equipment: The thermal control subsystem shall incorporate the necessary controls, instrumentation and/or auxiliary equipment needed to sense the KOH outlet temperature from the primary heat exchanger and to control it within the range of 179°F to 189°F, e.g., an automatic valve on the water supply to the heat exchanger.

2.3.6.1 Power for Auxiliaries: Either DC or AC power will be available for energizing subsystem auxiliaries. DC power will be at a potential of 29 ±2 volts while the AC will be three phase 115 ±5 volts (line to neutral) at 400 cycles per second. The ultimate selection of which type power is used should be made on the basis of obtaining the most reliable and/or qualified components.

2.3.6.2 Pressure References: Two alternate types of pressure reference schemes for the overall fuel cell system will be investigated by Union Carbide Corporation. These are:

1. Use of individual absolute pressure reference standards on each pressure regulation device, and
2. Placing the entire system in a capsule which is maintained at an ambient pressure of 14 psia ±0.25 psia.

(Within thirty days after initiating work subcontractor should advise Union Carbide Corporation of the advantages or disadvantages of either scheme as far as the thermal control subsystem is concerned.)

2.4 General Information

2.4.1 KOH in Gas Streams: Except for avoiding materials which rapidly corrode in the presence of potassium hydroxide, the design of the thermal control subsystem should assume that there is no potassium hydroxide carried in the circulating hydrogen or oxygen streams.

However, the thermal control subsystem design report submitted to Union Carbide Corporation shall include a discussion of the consequences of a malfunction which would permit 20 ml/hr of 12 N KOH to be released into either or both of the circulating gas streams.

2.4.2 Materials

2.4.2.1 Exposed to KOH: All materials which will be exposed to the circulating KOH stream must be resistant to corrosion and nonpoisoning to the fuel cell system. Acceptable materials which fit these criteria are: nickel, most plastics, precious metal brazing alloys, sulfur-free ethylene propylene, and sulfur-free neoprene.

Obviously, the subcontractor cannot determine which materials are nonpoisoning to the fuel cell system. Therefore, the subcontractor shall submit to Union Carbide a list of all materials (including their chemical analysis, if alloys) which will be exposed to KOH in the thermal control subsystem. No weight estimates or strength calculations shall be made until written approval of the materials is received. Union Carbide Corporation will wire such approval or disapproval within 24 hours after receipt of a request.

2.4.2.2 Gas and Condensate System: No aluminum or other material which corrodes rapidly in the presence of KOH shall be used in the gas, condensate or coolant systems. Magnesium, nickel, plastics, stainless steel, etc. are typical acceptable materials for these systems.

2.4.3 Design Considerations: Each of the components of the thermal control subsystem shall be designed to obtain the minimum weight and volume configuration consistent with the environmental and operational specifications set forth in this specification.

2.4.4 Properties of KOH: In all design calculations the physical properties of KOH supplied by Union Carbide Corporation should be used.

2.4.5 Overall System Schematic: Union Carbide Corporation will supply the overall system schematic for reference.

2.4.6 Mounting Brackets: Mounting brackets and/or shock absorbers, if required, shall be included in the design of each of the components in the thermal control subsystem. The subcontractor and Union Carbide Corporation shall coordinate this portion of the design so that the components will mount into the overall system.

2.4.7 Interconnecting Line Sizes: Within 15 days after the subcontractor initiates work, Union Carbide Corporation will advise him of the interconnecting line sizes for the H_2, O_2, and KOH streams. Within the same time period the subcontractor shall recommend line sizes for the coolant streams. Each of the thermal control subsystem components shall include connections which will permit removal of the component from the system.

2.4.8 Reliability: Although formal reliability analysis of the thermal control subsystem is not required under the present contract, the design should consider that ultimately such work will be required with the goal of space qualifying (for unmanned missions only) the resultant hardware.

2.4.9 Instrumentation: The design, e.g., source list, drawings, etc., of the thermal control subsystem shall not include any instrumentation whose sole purpose is to provide telemetry signals which could be used to monitor performance of the subsystem during a mission.

However, in the final thermal control subsystem design report submitted to Union Carbide Corporation the subcontractor shall include a list of recommended parameters which should be monitored in order to permit malfunction analysis during a mission.

DISTRIBUTION LIST NAS3-9430

	No. Copies
National Aeronautics & Space Administration Washington, D. C. 20546	
Attention: Ernst M. Cohn, Code RNW	1
G. F. Esenwein, Code MAT	1
A. M. Greg Andrus, Code FC	1
T. Albert, Code MLT	1
Office of Technology Utilization	1
National Aeronautics & Space Administration Scientific and Technical Information Facility Post Office Box 33 College Park, Maryland 20740	
Attention: NASA Representative	2 + 1 reproducible
National Aeronautics & Space Administration Goddard Space Flight Center Greenbelt, Maryland 20771	
Attention: Thomas Hennigan, Code 716.2	1
National Aeronautics & Space Administration Langley Research Center - Langley Station Hampton, Virginia 23365	
Attention: John Patterson	1
National Aeronautics & Space Administration Lewis Research Center 21000 Brookpark Road Cleveland, Ohio 44135	
Attention: B. Lubarsky, Mail Stop 500-201	1
M. J. Saari, Mail Stop 500-202	1
H. J. Schwartz, Mail Stop 500-202	1
J. E. Dilley, Mail Stop 500-309	1
N. D. Sanders, Mail Stop 302-1	1
J. S. Fordyce, Mail Stop 302-1	1
R. R. Miller, Mail Stop 500-202	1
Technology Utilization Office, Mail Stop 3-19	1
W. A. Robertson, Mail Stop 500-202	2
V. Hlavin, Mail Stop 3-14 (Final only)	1
Library, Mail Stop 60-3	1
J. M. McKee, Mail Stop 500-202	1
Report Control, Mail Stop 5-5	1
National Aeronautics & Space Administration George C. Marshall Space Flight Center Huntsville, Alabama 35812	
Attention: Mr. Charles Graff, R-ASTR-EAP	1
Mr. Richard Boehme, R-ASTR-E	1
National Aeronautics & Space Administration Ames Research Center - Pioneer Project Moffett Field, Mountain View, Calif. 94035	
Attention: John Rubenzer	1

DISTRIBUTION LIST NAS3-9430

	No. Copies
National Aeronautics and Space Administration Manned Spacecraft Center Houston, Texas 77001	
Attention: William R. Dusenbury	1
F. E. Eastman (EE-4)	1
Hoyt McBryar (EP-5, Bldg. 16)	1
Jet Propulsion Laboratory 4800 Oak Grove Drive Pasadena, California 91103	
Attention: Aiji Uchiyama	1
National Aeronautics and Space Administration Electronics Research Center 575 Technology Square Cambridge, Massachusetts 02139	
Attention: Dr. S. Gilman	1
Department of the Army	
U. S. Army Engineer R & D Laboratories Fort Belvoir, Virginia 22060	
Attention: Energy Conversion Research Lab	1
Commanding General U. S. Army Electronics Command Power Sources Branch Fort Monmouth, New Jersey 07703	
Attention: Code AMSEL-KL-P	1
Harry Diamond Laboratories Room 300, Building 92 Connecticut & Van Ness, N.W. Washington, D. C. 20438	
Attention: Nathan Kaplan	1
U. S. Army Natick Laboratories Clothing & Organic Materials Division Natick, Massachusetts 01760	
Attention: Leo A. Spano	1
Department of the Navy	
Office of Naval Research Department of the Navy Washington, D. C. 20360	
Attention: Dr. Ralph Roberts/H. W. Fox	1
U. S. Naval Research Laboratory Washington, D. C. 20390	
Attention: Dr. J. C. White, Code 6160	1

DISTRIBUTION LIST NAS3-9430

	No. Copies
Commander, Naval Ship Systems Command Department of the Navy Washington, D. C. 20360 Attention: B. B. Rosenbaum, Code 03422	1
Commander, Naval Ship Systems Command Department of the Navy Naval Ship Engineering Center Washington, D. C. 20360 Attention: C. F. Viglotti, Code 6157	1
Naval Ordnance Laboratory Department of the Navy Corona, California 91720 Attention: William C. Spindler, Code 441	1
Naval Ordnance Laboratory Department of the Navy Silver Spring, Maryland 20910 Attention: Phillip B. Cole, Code 232	1
U. S. Navy Marine Engineering Lab Special Projects Division Annapolis, Maryland 21402 Attention: J. H. Harrison	1
Department of the Air Force	
Aeronautical Systems Division Flight Vehicle Power Branch Air Force Aero Propulsion Laboratory Wright-Patterson Air Force Base, Ohio 45433 Attention: J. E. Cooper, Code APIP-2	1
Air Force Cambridge Research Laboratory L. G. Hanscom Field - CRE Bedford, Massachusetts 01731 Attention: F. X. Doherty E. Raskind (Wing F)	1 1
Rome Air Development Center Griffiss AFB, New York 13442 Attention: Frank J. Mollura (RASSM)	1
Other Government Agencies	
Army Reactors, DRD U. S. Atomic Energy Commission Washington, D. C. 20545 Attention: D. B. Hoatson	1

DISTRIBUTION LIST NAS3-9430

	No. Copies
Office, DDR&E: Sea Warfare Systems The Pentagon Washington, D. C. 20301 Attention: G. B. Wareham	1
Office of Technical Services Department of Commerce Washington, D. C. 20009	1
Clearing House 5285 Park Royal Road Springfield, Virginia 22151	1
Bureau of Mines 4800 Forbes Avenue Pittsburgh, Pennsylvania 15213 Attention: Mr. D. Bienstock	1
Private Industry	
Aeronutronic Division Philco Corporation - Ford Road Newport Beach, California 92663 Attention: Technical Information Services	1
AiResearch Manufacturing Company 9851 Sepulveda Blvd. Los Angeles, California 90009 Attention: Mr. D. S. Davis	1
Allis-Chalmers Manufacturing Company 1100 South 70th Street Milwaukee, Wisconsin 53214 Attention: J. W. McNeil, Manager Marketing Research Division	1
Allis-Chalmers Manufacturing Company Research Division P. O. Box 512 Milwaukee, Wisconsin 53201 Attention: Dr. P. A. Joyner	1
Allison Division General Motors Corporation Indianapolis, Indiana 46206 Attention: Dr. Robert E. Henderson	1
American Machine & Foundry Research & Development Division 689 Hope Street Springdale, Connecticut 06879 Attention: Dr. L. H. Shaffer	1

DISTRIBUTION LIST NAS3-9430

	No. Copies
American Cyanamid Company 1937 West Main Street Stamford, Connecticut 06901 Attention: Dr. R. G. Haldeman	1
Aerospace Corporation P. O. Box 95085 Los Angeles, California 90045 Attention: Technical Library Acquisitions Group	1
Arthur D. Little Incorporated Acorn Park Cambridge, Massachusetts 02140 Attention: Dr. Ellery W. Stone	1
Atlantic Refining Company 500 South Ridgeway Avenue Glenolden, Pennsylvania 19036 Attention: Dr. Harold Shalit	1
Atomics International Division North American Aviation Incorporated 8900 DeSoto Avenue Canoga Park, California 91304 Attention: Dr. H. L. Recht	1
Battelle Memorial Institute 505 King Avenue Columbus, Ohio 43201 Attention: Dr. C. L Faust	1
Bell Telephone Laboratories Incorporated Murray Hill, New Jersey 07971 Attention: Mr. U. B. Thomas	1
ChemCell Incorporated 150 Dey Road Wayne, New Jersey 07470 Attention: Mr. Peter D. Richman	1
Clevite Corporation Mechanical Research Division 540 East 105 Street Cleveland, Ohio 44108 Attention: D. J. Berger	1
Dynatech Corporation 17 Tudor Street Cambridge, Massachusetts 02139 Attention: R. L. Wentworth	1

DISTRIBUTION LIST NAS3-9430

	No. Copies
Douglas Aircraft Company, Inc. Astropower Laboratory 2121 Campus Drive Newport Beach, California 92663 Attention: Dr. Carl Berger	1
Electrochimica Corporation 1140 O'Brien Drive Menlo Park, California 94025 Attention: Dr. Morris Eisenberg	1
Electro-Optical Systems, Inc. 300 North Halstead Street Pasadena, California 91107 Attention: Mr. Kline	1
Engelhard Industries, Inc. 497 Delancy Street Newark, New Jersey 07105 Attention: Dr. J. G. Cohn	1
Esso Research and Engineering Company Government Division P. O. Box 8 Linden, New Jersey 07036 Attention: Dr. C. E. Heath	1
The Franklin Institute Benjamin Franklin Parkway Philadelphia, Pennsylvania 19103 Attention: Robert Goodman	1
Garrett Corporation 1625 Eye Street, N. W. Washington, D. C. 20013 Attention: Mr. Bowler	1
General Dynamics/Convair P. O. Box 1128 San Diego, California 92112 Attention: R. P. Mikkelson, Electrical Systems Department 988-7	1
General Electric Company Direct Energy Conversion Operations 930 Western Avenue Lynn, Massachusetts 01901 Attention: P. Schratter	1
General Electric Company Research & Development Center P. O. Box 8 Schenectady, New York 12301 Attention: Dr. H. Liebhafsky	1

DISTRIBUTION LIST NAS3-9430

	No. Copies
General Electric Company 777 - 14th Street, N. W. Washington, D. C. 20005 Attention: P. C. Hargraves	1
General Motors Corporation P. O. Box T Santa Barbara, California 93102 Attention: Dr. C. R. Russell	1
General Motors Corporation Research Laboratories Electrochemistry Department 12 Mile & Mound Roads Warren, Michigan 48090 Attention: Dr. S. E. Beacom	1
Globe-Union Incorporated P. O. Box 591 Milwaukee, Wisconsin 53201 Attention: J. D. Onderdonk	1
Hughes Research Laboratories Corporation 3011 Malibu Canyon Road Malibu, California 90265 Attention: T. M. Hahn	1
Ionics Incorporated 65 Grove Street Watertown, Massachusetts 02172 Attention: Dr. Werner Glass	1
Institute for Defense Analyses Research & Engineering Support Division 400 Army-Navy Drive Arlington, Virginia 22202 Attention: Dr. G. C. Szego Dr. R. Briceland	1 1
Institute of Gas Technology State and 34th Streets Chicago, Illinois 60616 Attention: Dr. B. S. Baker	1
Johns Hopkins University Applied Physics Laboratory 8621 Georgia Avenue Silver Spring, Maryland 20910 Attention: R. Cole	1

DISTRIBUTION LIST NAS3-9430

	No. Copies
Johns-Manville R&E Center P. O. Box 159 Manville, New Jersey 08835 Attention: J. S. Parkinson	1
Leesona Moos Laboratories Lake Success Park Community Drive Great Neck, New York 11021 Attention: Dr. A. Moos	1
Lockheed Missiles and Space Company Technical Information Center 3251 Hanover Street Palo Alto, California 93404	1
McDonnell Aircraft Corporation P. O. Box 516 St. Louis, Missouri 63166 Attention: Project Gemini Office	1
Midwest Research Institute 425 Volker Boulevard Kansas City, Missouri 64110 Attention: Physical Science Library	1
Monsanto Research Corporation Boston Laboratories Everett, Massachusetts 02149 Attention: Dr. J. O. Smith	1
Monsanto Research Corporation Dayton Laboratory Dayton, Ohio 45407 Attention: Librarian	1
North American Aviation Company S&ID Division Downey, California 90241 Attention: Dr. James Nash	1
Oklahoma State University Stillwater, Oklahoma 74075 Attention: Prof. William L. Hughes	1
Power Information Center University of Pennsylvania Moore School Building 200 South 33rd Street Philadelphia, Pennsylvania 19104	1

DISTRIBUTION LIST NAS3-9430

	No. Copies
Pratt & Whitney Aircraft Division United Aircraft Corporation East Hartford, Connecticut 06108 Attention: Librarian	1
Radio Corporation of America Astro Division P. O. Box 800 Hightstown, New Jersey 08520 Attention: Dr. Seymour Winkler	1
Rocketdyne 6633 Canoga Avenue Canoga Park, California 91304 Attention: Library, Dept. 086-306 Zone 2	1
Speer Carbon Company Research & Development Laboratories Packard Road at 47th Street Niagara Falls, New York 14304 Attention: W. E. Parker	1
Stanford Research Institute 820 Mission Street South Pasadena, California 91108 Attention: Dr. Fritz Kalhammer	1
Texas Instruments Incorporated 13500 North Central Expressway Dallas, Texas 75222 Attention: Dr. Issac Trachtenberg	1
Thiokol Chemical Corporation Reaction Motors Division Denville, New Jersey 07834 Attention: Dr. D. J. Mann	1
TRW Incorporated 23555 Euclid Avenue Cleveland, Ohio 44117 Attention: Dr. R. A. Wynveen	1
TRW Systems One - Space Park Redono Beach, California 90278 Attention: Dr. A. Krausz	1
Tyco Laboratories Incorporated Bear Hill - Hickory Drive Waltham, Massachusetts 02154 Attention: Dr. A. C. Makrides	1

DISTRIBUTION LIST NAS3-9430

	No. Copies
Unified Science Associates, Inc. 826 South Arroyo Parkway Pasadena, California 91105 Attention: Dr. S. Naiditch	1
University of California Space Science Laboratory Berkeley, California 94701 Attention: Prof. Charles W. Tobias	1
University of Pennsylvania Electrochemistry Laboratory Philadelphia, Pennsylvania 19104 Attention: Prof. John O'M. Bockris	1
University of Pennsylvania Institute for Direct Energy Conversion 260 Towne Building Philadelphia, Pennsylvania 19104 Attention: Dr. Manfred Altman	1
University of Toledo Toledo, Ohio 43606 Attention: Dr. A. Krohn	1
The Western Company RCA Building - Suite 802 Washington, D. C. 20006 Attention: R. T. Fiske	1
Western Reserve University Department of Chemistry Cleveland, Ohio 44106 Attention: Prof. Ernest Yeager	1
Westinghouse Electric Corporation Research and Development Center Churchill Borough Pittsburgh, Pennsylvania 15235 Attention: Dr. A. Langer	1
Whittaker Corporation NARMCO R&D Division 3540 Aero Court San Diego, California 92123 Attention: Dr. M. Shaw	1

DISTRIBUTION LIST NAS3-9430

	No. Copies
Yardney Electric Corporation 40 Leonard Street New York, New York 10013 Attention: Dr. George Dalin	1
Zaromb Research Corporation 376 Monroe Street Passaic, New York 07055	1